NAVAL POSTGRADUATE SCHOOL
MONTEREY, CALIFORNIA

THESIS

EXISTING AND EMERGING MARITIME
SURVEILLANCE TECHNOLOGIES

by

Gary A. Burkholder

September 1995

Thesis Advisor: Phillip E. Pace

Approved for public release; distribution is
unlimited

REPORT DOCUMENTATION PAGE			Form Approved OMB No. 0704-0188

Public reporting burden for this collection of information is estimated to average 1 hour per response, including the time for reviewing instructions, searching existing data sources, gathering and maintaining the data needed, and completing and reviewing the collection of information. Send comments regarding this burden estimate or any other aspect of this collection of information, including suggestions for reducing this burden, to Washington Headquarters Services, Directorate for Information Operations and Reports, 1215 Jefferson Davis Highway, Suite 1204, Arlington, VA 22202-4302, and to the Office of Management and Budget, Paperwork Reduction Project (0704-0188), Washington, DC 20503.

1. AGENCY USE ONLY (Leave blank)	2. REPORT DATE September 1995	3. REPORT TYPE AND DATES COVERED Master's Thesis	

4. TITLE AND SUBTITLE
EXISTING AND EMERGING MARITIME SURVEILLANCE
TECHNOLOGIES

5. FUNDING NUMBERS

6. AUTHOR(S)

Burkholder, Gary A.

7. PERFORMING ORGANIZATION NAME(S) AND ADDRESS(ES)

Naval Postgraduate School
Monterey, CA 93943-5000

**8. PERFORMING ORGANIZATION
REPORT NUMBER**

9. SPONSORING / MONITORING AGENCY NAME(S) AND ADDRESS(ES)

**10. SPONSORING / MONITORING
AGENCY REPORT NUMBER**

11. SUPPLEMENTARY NOTES
The views expressed in this thesis are those of the author and do not reflect the official policy or position of the Department of Defense or the United States Government.

12a. DISTRIBUTION / AVAILABILITY STATEMENT

Approved for public release, distribution is unlimited.

12b. DISTRIBUTION CODE

13. ABSTRACT (Maximum 200 words)

This paper presents an assessment of present and near-future maritime surveillance technologies. Radar, optical and infrared sensor systems are each discussed. Thirty-two major domestic and foreign manufacturers' market position, current products and their applications are reviewed. State-of-the-art research is presented and analyzed to see in what direction the future of maritime surveillance is headed. In examining current systems and those being researched, rapid signal processing, data fusion, interpretation and dissemination constitute the major challenges and provide the most opportunities for improvement.

14. SUBJECT TERMS

Maritime surveillance, radar, infrared, photography

15. NUMBER OF PAGES
136

16. PRICE CODE

17. SECURITY CLASSIFICATION OF REPORT Unclassified	18. SECURITY CLASSIFICATION OF THIS PAGE Unclassified	19. SECURITY CLASSIFICATION OF ABSTRACT Unclassified	20. LIMITATION OF ABSTRACT UL

NSN 7540-01-280-5500

Standard Form 298 (Rev. 2-89)
Prescribed by ANSI Std. Z39-18
298-102

ii

EXISTING AND EMERGING
MARITIME SURVEILLANCE TECHNOLOGIES

Gary A. Burkholder
Lieutenant, United States Navy
B.E. Vanderbilt University, 1987

Submitted in partial fulfillment of the
requirements for the degree of

MASTER OF SCIENCE IN AERONAUTICAL ENGINEERING

from the

NAVAL POSTGRADUATE SCHOOL
September, 1995
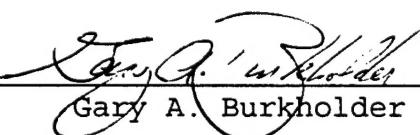
Author: _____
Gary A. Burkholder

Approved by: _____
Phillip E. Pace, Thesis Advisor

_____
Oscar Biblarz, Second Reader
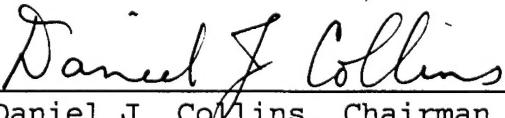
_____
Daniel J. Collins, Chairman
Department of Aeronautics and Astronautics

iii

ABSTRACT

This paper presents an assessment of present and near-future maritime surveillance technologies. Radar, optical and infrared sensor systems are each discussed. Thirty-two major domestic and foreign manufacturers' market position, current products and their applications are reviewed. State-of-the-art research is presented and analyzed to see in what direction the future of maritime surveillance is headed. In examining current systems and those being researched, rapid signal processing, data fusion, interpretation and dissemination constitute the major challenges and provide the most opportunities for improvement.

v

vi

TABLE OF CONTENTS

LIST OF FIGURES

ix

x

LIST OF TABLES

LIST OF ACRONYMS AND ABBREVIATIONS

AESA	Active Element electronically Scanned phased Array
ATC	Air Traffic Control
AVIRIS	Airborne Visible-Infrared Imaging Spectrometer
ASP	Alaska Synthetic Aperture Radar Processor
ADC	Analog/Digital Converter
AGC	Automatic Gain Control
ATR	Automatic Target Recognition
CNR	Clutter to Noise Ratio
CMOS	Complimentary Metal-Oxide Semiconductor
CFAR	Constant False Alarm Rate
DAC	Digital/Analog Converter
DDS	Direct Digital Synthesis
DPCA	Displaced Phase Center Antenna
EMI	Electromagnetic Interference
ECCM	Electronic Counter-Counter Measures
ESA	Electrostatic Amplifier
ECA	Electrostatic Combined Amplifier
EIA	Extended Interaction Amplifier
ECS	Extended Chirp Scaling
FPA	Focal Plane Array
FOPAIR	FOcused Phased Array Imaging Radar
f_s	Frequency Threshold
GLR	Generalized Likelihood Ratio
GSSR	Goldstone Solar System Radar
HUD	Heads-Up Display
HBAR	High overtone Bulk Acoustic Resonator
HPA	High Power Amplifier
I/Q	In-phase/Quadrature
IR	Infrared
IOGW	Integrated Optical Guided Wave
IC	Integrated Circuit
IMTF	Interferomic Moving Target Focusing
IF	Intermediate Frequency
ISAR	Inverse Synthetic Aperture Radar

JDL	Joint Domain Localized
LCC	Life Cycle Cost
LO	Local Oscillator
MTBF	Mean Time Between Failure
MESFET	Metal Semiconductor Field Effect Transistor
MMIC	Monolithic Microwave Integrated Circuits
MTI	Moving Target Indicator
MCM	Multi-chip Module
MHT	Multi-Hypothesis Tracking
MBSD	Multiband Sigma Delta
NRL	Naval Research Laboratory
PIRATE	Passive InfraRed Airborne Tracking Equipment
PGA	Phase Gradient Autofocus
PAE	Power Added Efficiency
P_d	Probability of Detection
P-HEMT	Pseudomorphic High Electron Mobility Transistor
PRI	Pulse Repetition Interval
R&D	Research and Development
RTD&E	Research, Testing, Development and Evaluation
SRC	Secondary Range Compression
STC	Sensitivity Time Control
SAC	Shift And Correlate
SD	Sigma Delta
SNR	Signal to Noise Ratio
STP	Space Time Processing
SAW	Surface Acoustic Wave
SAR	Synthetic Aperture Radar
TE	Thermo-Electric
T/R	Transmitter/Receiver
TSVQ	Tree Structured Vector Quantizer
VQ	Vector Quantizer
VCO	Voltage Controlled Oscillator

ACKNOWLEDGMENT

I. INTRODUCTION

A. BACKGROUND

Maritime surveillance is the process of monitoring traffic in, on and above the oceans. It is done for a number of reasons including, but not limited to maintaining exclusive economic zones, ensuring freedom of navigation and tracking oil spills, icebergs, and illegal drug traffic. Those being monitored may be friendly, neutral or even hostile. For brevity and simplicity, this thesis is limited to traffic on and above the seas' surface.

Each surveillance platform has its own advantages and disadvantages. Ships possess virtually unlimited endurance, but are usually limited to line-of-sight range. Airborne platforms usually have fairly long range and mobility, but they lack endurance. Shore facilities are capable of very long ranges and endurance, but obviously, lack mobility. Satellites have many of the advantages and few disadvantages. However, they are typically national strategic assets and often closely controlled. Thus, they may lack flexibility and not provide timely information to the on-scene commander down at the tactical level. High sea states and cloud cover may also limit surveillance capability.

During the Cold War, maritime surveillance mostly concerned "blue water" operations; those taking place far from shore. During the past five years, however, there has been a shift to littoral or "brown water" operations within 100 nm of shore.

1

B. PRINCIPAL CONTRIBUTIONS

This thesis presents an assessment of present and near-future maritime surveillance capabilities. Radar, optical and infrared sensors are each discussed. Major domestic and foreign manufacturers' current products and their applications are reviewed. State-of-the-art research is presented and analyzed to see in what direction the future of maritime surveillance is headed.

Data were obtained from a variety of sources. R&D and company marketing personnel provided information and insight into their areas of expertise. This material was compiled into tables presented elsewhere in the thesis. Corroborative information from defense and industry trade publications was scrutinized, particularly for manufacturing and acquisition news.

C. THESIS OUTLINE

Chapter II reviews the current state-of-the-art in maritime surveillance technologies. It is broken down into radar, optic and infrared sections. Chapter III addresses the major "players" in maritime surveillance. Manufacturers and their relevant products are reviewed and analyzed. Noteworthy civilian and military research institutions are also discussed. Chapter IV describes the various maritime surveillance missions, their requirements and the state-of-the-art technologies that are most likely to fulfil those requirements. Chapters V contains conclusions and a summary.

2

II. STATE-OF-THE-ART

A. RADAR TECHNOLOGY

Stringent military threat requirements have historically been the driving force for radar development. In the near future however, the smaller military market will no longer dominate radar research and development (R&D). Instead, commercial opportunities will provide the bulk of the sales and therefore, decide the direction of R&D. Future civil Air Traffic Control (ATC) radar systems will demand the capability to safely handle increased traffic flow in excess of current radar capability. Although the driving requirements for civil and mobile military radars contain key differences, virtually all the features that apply to ATC radars have parallel applications to military radars, whether ship, shore, aircraft or space mounted. The auto industry is pursuing low-cost collision avoidance radars. When this research comes to fruition, the sheer numbers of small, lightweight radars will have a huge impact on the radar industry. [Ref.1]

1. Transmitters & Receivers

State-of-the-Art radars are characterized by their compact, synergistic combination of several different technologies. For clarity in analysis, however, the systems can be broken down into their individual components.

a. *MMICs*

The most up-to-date systems use tiny Gallium Arsenide or GaAs/AlGaAs Pseudomorphic High Electron Mobility Transistor (P-HEMT) monolithic technology. They are based on monolithic microwave integrated circuits (MMICs), which are assembled to form transmitter/receiver modules, each one on a single chip. A large number (up to ~2000) of these modules are arranged on an advanced active array antenna, blurring the distinction between transmitter, receiver and antenna. Each module provides both radiated transmit power and low noise amplification upon reception, as well as phase shifters to electronically scan the antenna beam. [Ref. 2]

Table 1 shows transmitter/receiver (T/R) module development in terms of capability, size, cost and reliability. During the late 1980s and early 90s, laboratory T/R module packages measuring 200 mm^2 were the norm. Though specific designs varied slightly, each one consists of five to six circuits on several chips, typically including a VCO, six-bit phase shifter, transmitter amplifier, receiver amplifier and receiver mixer. The chips are a multi-layer structure composed of a wafer of metal and interlayered dielectrics. "Via holes" are usually etched through the dielectric layers to ground the elements. [Ref. 3]

4

Parameter	1983	1987	1990
Peak Output Power (watts)	~1	2	5
MTBF (hours)	60,000	60,000	200,000
Volume (in³)	1.56	0.69	0.39
Weight (oz.)	1.84	1.54	0.70
Cost (1985 $)	12,000	8,000	3,000

Table 1; T/R Module Evolution [Ref. 4]

In 1993, researchers at TRW produced a T/R module on a single 24.8 mm² InGaAs/AlGaAs chip using 0.1 um P-HEMT process technology [Ref. 5]. Shrinking both the circuit and chip sizes was aggressively pursued throughout the development. Since amplifiers are traditionally large, reducing their size has the biggest impact on module size and subsequently, cost. Once T/R modules are batch processed on wafers to form a tile, multiple tiles are assembled to fit any desired radar configuration. The tiles are attached to a backplane that provides the mechanical support. Fiber optic links can be used to manifold the transmit, receive and control signals to and from the subarray tiles. In addition, the backplane contains the necessary cooling channels. Since the array is thin and lightweight, it can be integrated onto the skin of an aircraft or other surveillance platform. [Ref. 6]

GaAs/AlGaAs P-HEMTs feature lower noise than GaAs at low frequencies because their 1/f corner frequency is much

5

lower [Ref. 7]. Therefore, using the same design approach, the oscillator will show less FM noise than a metal semiconductor field effect transistor (MESFET) oscillator at frequencies close to the carrier. Performance of the single chip is similar to that of its "older brother", the GaAs MESFET chip, but with improved sensitivity due to superior noise characteristics. Thus, P-HEMT technology appears to offer better performance over MESFET, but is slightly less mature and has not yet been demonstrated in production. It is proposed that P-HEMT technology be substituted when considered sufficiently developed for production [Ref.1].

The processes required to manufacture traditional frequency sources using Gunn oscillators is labor intensive and does not lend itself well to low production costs [Ref.1]. Due to these limitations, MMIC technology finds a unique opportunity to be inserted into large volume production programs in the near future. Use of microwave multi-chip module (MCM) and fiber optic technologies can provide the affordability, small size, wide bandwidth, flexibility, EMI resistance, and manufacturability needed for the next generation of shared conformal aperture radars utilizing MMIC technology for active arrays. MMIC circuits have exceptional prime power efficiency characteristics; Power Added Efficiencies (PAE) are about 40% [Ref. 8]. They also have the ability to vary the output power. Various experimental results to date typically demonstrate power levels exceeding 7 watts per single-chip T/R module with bandwidths of

6

approximately 550 MHz [Ref. 9]. Finally, because of the sheer number of T/R modules, array failure (if or when it does happen) is characterized by a graceful degradation of capability instead of sudden total failure. However, MMIC yield is often limited by wafer processing stability. Another design issue involves tuning; unlike conventional designs, MMICs can't be tuned after manufacture. Thus, the design must meet the required specifications the first time it's tested. Finally, the heavy cooling requirements for active array antennas puts a tremendous premium on achieving significantly higher power-added efficiency.

ATC systems depend on many unique and costly radars because current radar technology is limited to narrow band operation (~10% of operating frequency)[Ref. 8]. The advent of the wideband active array (octave bandwidth) makes it possible to extend the MMIC chip capability to cover the C through Ku bands. Thus, many ATC functions can be combined into one radar, avoiding the "seams" or skipped regions of coverage. Currently, X-Ku-band MMIC chips (8-14 GHz) already being developed by ITT make possible an airport terminal area surveillance system capable of performing three of the primary ATC functions [Ref. 8]. The same chips can easily be adapted for military surveillance radars as well.

The development of cost effective T/R modules to produce active arrays has been sought for over 30 years. Today, modules are becoming available that provide the performance capability to develop advanced radar systems at a

7

competitive cost. As the T/R module price approaches the $500 goal, active array radars will be the cost effective answer to ATC (and subsequently, military) requirements. Since many radars will have the same features, individual development programs will be less costly. Further, Life Cycle Costs (LCC) are half that of the tube type systems currently used by many ATCs. The LCC savings, coupled with the performance advantages make the fielding of MMIC chip-based active array systems an eventual certainty [Ref. 8]. Still, to ensure the commercial reality of active, T/R module-based radars, four areas of study must be pursued further [Ref. 8]:

- efficiency
- noise factor reduction
- reliability
- cost(assembly & packaging technology, large-scale manufacturing and testing)

b. *Magnetrons*

Published research on magnetrons appears to be overshadowed by other, more "exciting" topics. Nonetheless, they remain very important for several reasons, particularly in experimental radars. Magnetrons can be made small and efficient at millimeter-wave frequencies. They also tend to be very effective in applications which require a high peak power/low duty cycle format [Ref. 10]. Current state-of-the-art magnetrons using cross-field amplifier technology are achieving 10 MW peak and 100 kW average power @ 1 GHz, with

8

mean time between failure (MTBF) of 100,000 hours [Ref. 11].

One criticism of magnetrons is their tendency toward erratic performance, often because of inadequate consideration of fault condition operations such as power surges. This is a particularly critical concern in millimeter wave tubes where internal geometry is very small and arcing events, if not carefully controlled, can be quite damaging to the tubes. One solution is to minimize the output capacitance, reducing energy available during tube arcs and avoiding damage. Other limitations on magnetron performance involve frequency and spectral signature stability; both of which are strongly influenced by power supply and modulator design. [Ref. 10]

New low-noise, self-protecting microwave amplifiers are under development using electrostatic amplifiers (ESAs). When combined with magnetron oscillators, ESAs provide compact transmitters and are being used in ground-based pulse-Doppler radar systems. They can provide low noise figures (.7-4 dB @ .4-14 GHz), wide dynamic range, linear amplitude and phase characteristics, and the ability to handle unexpected power inputs (up to 500 kW). The recovery to maximum sensitivity after an input overload is typically 10-50 ns. All this is accomplished without additional protection (ie: gas discharge T/R tubes, diode limiters or switches). Thus, the ESA noise figure almost completely defines radar receiver sensitivity. [Ref. 12]

9

ESA theory is far from complete. However, the maximum allowed microwave power level in the amplifier input is determined by the electric strength of the ESA input circuit and the breakdown of the capacity gap of the input resonator. Additionally, a crucial requirement for ESA operation is a carefully controlled magnetic field. Recent ESA designs use samarium-cobalt permanent magnets for smaller size, weight and improved efficiency. [Ref. 12]

In order to increase gain, ESAs have been further developed with integral transistor amplifiers; these devices are called electrostatic combined amplifiers (ESCAs). Additionally, devices called "potentialotrons" have been developed which combine magnetrons with ESAs. Potentialotrons join the functions of power-pulsed oscillators, low-noise amplifiers, and rapid transmit/receive switches. [Ref. 12]

c. *Klystrons*

There is an increasing interest in high-PRF pulse Doppler radars for many uses, especially ground-based surveillance systems. Typically, the target range is ambiguous and its weak return is embedded in heavy clutter from a closer range. A medium power, gridded, pulsed klystron amplifier is an attractive choice for the final amplification of a pulse Doppler transmitter in these applications, especially if large values of instantaneous bandwidth are not required. These klystrons are available with average powers in excess of 6 kW, tunable over 10% BW, operate through the

10

Ka-Band, and are typically gridded. They offer low cost, high average power, low phase noise, and ease of modulation [Ref. 13]. Significantly more impressive are alloy-doped klystrons which may achieve 95 MW peak, 3MW average power @ 1 GHz with MTBFs of 20,000 hours [Ref. 11].

When carefully designed, klystron amplifiers exhibit long lives in many applications. However, the fragile grid is unforgiving of positive voltage applications without full beam voltage. The most stressing condition involves the development of an arc in the tube structure. While this is infrequent, arcs do occur and protection circuitry must be provided.

Crowbarring is an attractive method of tube protection. This involves spark gap circuits which discharge the power supply. These circuits must be at least critically damped to prevent oscillatory discharge and subsequent opening of the gaps upon voltage reversal. They must also provide some place for the stored energy to be dissipated. These requirements are satisfied by connecting series resistors between the gaps and the energy storage capacitors. [Ref. 13]

Other klystron research is being driven by airborne millimeter-wave radars used to detect cloud microstructure and ice/water composition. Pulsed polarimetric millimeter-wave radars that use extended interaction klystron amplifier (EIA) and oscillator tubes are popular for their compact size, high sensitivity, and highly directive antennas. The University of Massachusetts has developed two polarimetric

11

radars using EIA tubes for transmission of high peak power pulses. The first is a 95 GHz coherent radar which measures the complex scattering matrix of a target by alternate transmission of vertical and horizontal polarized pulses. The second is a noncoherent pulsed polarimetric 225 GHz radar which directly senses the target by six differently polarized waves. It uses an EIA that generates a 60 W peak power pulse. [Ref. 14]

One of the most interesting platforms involving klystron research is the Goldstone Solar System Radar (GSSR). In addition to its primary purpose of tracking spacecraft, the system provided the first topographical map of the planet Venus. It is used for radio astronomy at L-K-Bands and radar astronomy at X-Band. Recently, the GSSR transmitter was upgraded with two new state-of-the-art VKX-7864A Klystron Amplifiers. Each tube delivers 250 kW @ 8510 MHz. Features include a saturated gain of 50 dB and 45% electronic efficiency. Frequency band edges are 8500-8520 MHz with a power variation of 0.25 dB over the 20 MHz. By cryogenically cooling a major portion of the receive feed components, the receiver noise temperature is reduced from 18.0 to 14.7 K. Overall, a 2.0 dB improvement is achieved [Ref. 15]. Each klystron consists of an input cavity, four buncher cavities and an output cavity. Heavy emphasis is placed on improved reliability; a reduction in the maximum electric field gradient in the gun region from 350 to 225 kV/inch eliminates arcing problems experienced in previous designs [Ref. 15].

12

Additionally, each klystron is provided with an arc detector at the window and a reverse power coupler. In the event of a fault, these monitor and remove the RF drive before permanent damage can occur. [Ref. 16]

Combined output for the two VKX-7864A's is about 500 kW, but because of losses due to combining the waveguide transmission, radiated power at the feedhorn is 450 kW [Ref. 15]. High power alone, however, will not provide the desired CW radar transmitter capabilities. If this were the case, it might be more easily obtained with an oscillator rather than an amplifier. Using an amplifier allows dynamic control of amplitude and phase and eliminates the need for phase locking an oscillator to a control signal. [Ref. 17]

Two future GSSR system upgrades are proposed; the first is implementation of a single horn HEMT transmit/receive system to reduce the switching time between transmit and receive portions of the cycle. This is for near-earth observations and has applications in maritime surveillance. The second is a doubling of the transmitter power to 1 MW using four 250 kW klystrons. Each pair feeds a separate feedhorn. The power from each feedhorn is phased and combined using a polarization grid. [Ref. 17]

d. Travelling Wave Tubes

Travelling wave tubes (TWTs) are characterized by high gain, large bandwidth, high operating voltages and low efficiencies. Typical capabilities of current production TWTs

13

are 700 kW @ 1.3 GHz and 4.5 MW @ 5.65 GHz [Ref. 18]. Additionally, several Japanese organizations are researching mm-wave (43-45 GHz) TWTs [Ref. 19].

Relatively low efficiency is the principal drawback of TWTs. Two approaches are used to combat this. The first entails depressing the collector (operating the collector at a potential below the body). This improves efficiency at the expense of complexity. The second is velocity synchronization, wherein the potential of the last portion of the periodic structure is increased slightly. Combining these two approaches boosts TWT efficiency to ~60% [Ref. 18]. To further improve efficiency, new low dielectric, high thermal conductivity materials, such as diamond and boron nitride, are being investigated. Additionally, helix TWT efficiencies are increased by using helix velocity tapers on the output of the helix circuit. This allows close coupling between the electron beam and the helix in the last section, where power buildup is exponential [Ref. 11]. This method has applications in active phased array surveillance radars, where helix TWTs may be well suited due to their high power output.

e. *Receivers*

Millimeter-wave systems have been dominated by waveguide-based designs constructed from separately manufactured components. However, an integrated four-horn monopulse tracking receiver with intermediate frequency (IF) beam control is shown to perform comparably with waveguide

14

systems, but with much lower fabricating costs. It uses four IF signals to produce the monopulse sum and difference patterns for both the elevation and azimuth coordinates, using inexpensive low frequency signal processing components. The receiver is integrated on a single silicon chip and is based on a single 23 GHz local oscillator (LO) driving four separate phase-coherent 94 GHz subharmonic mixers at one fourth the RF or 23 GHz. This is low enough to allow the LO power to be produced and distributed with low losses using planar transmission lines. The LO is powered by a voltage controlled oscillator (VCO) using a commercially available HEMT, the NEC #NE32100. Because the mixers are driven by the same LO source, their IF signals are phase coherent. [Ref. 20]

Analysis shows 6-8 mW of LO power is needed to drive each subharmonic mixer or 24-32 mW to drive all four. With a typical conversion loss of 12-14 dB, the diode series resistance is an especially important parameter in determining performance limits of the second subharmonic mixer. VCO measurements indicate the output frequency is linear with a veractor bias of 0 to -15 V, tuning range of 250 MHz and an output power of 0.5 to 1 mW. The total conversion loss, L_{ct}, of the receiver is the measured IF power at 200 MHz into a 50 ohm load, divided by the total 94 GHz power incident on the horn aperture. The calculated mixer conversion loss is 19.5 dB and is dominated by the effects of the high series resistance. When combined with the 3.5 dB antenna losses,

15

this gives a total calculated conversion loss of 23 dB (~5-6 dB remains unaccounted for). [Ref. 20]

Multiple polarization receivers are another area of research. Detection is accomplished using a bank of k polarization filters, matched to equally spaced polarizations. By increasing the number of branches in the multi-polarization receiver, a constant performance level can be approached comparable to that of an "optimum" receiver [Ref. 21].

The performance of such a multipolarization receiver is evaluated in terms of false alarm and target detection probabilities. For both the multipolarization receiver with two branches and an optimum receiver, target detection probability (P_d) is a function of polarization. In a clutterless environment, the optimum receiver maintains a constant P_d value of 35.1%, independent of polarization. The two-branch multi-polarization receiver varies from 4.6% to 43.8% with an average of about 25%. The highest P_d values are obtained when clutter is completely polarized and its polarization completely mismatched with at least one of the filter polarizations. Lowest values are obtained for clutter orthogonal to that of target polarization. In the cluttered environment, the receiver's P_d is steady at 41.77%, excellent for all signal polarizations. [Ref. 21]

The main problem with this multi-polarization technique is the inability to estimate the linear transformation matrices in the polarization domain for the unknown polarization characteristics of received signals.

16

Still, this procedure receiver appears to be a viable approach in improving target detection in the presence of clutter, while approaching performance of the optimum dual polarization receiver for unpolarized targets in the clear. [Ref. 21]

Perhaps the most interesting receiver research involves effectively increasing its dynamic range. Modern air surveillance radars including ATC and AEW systems require receivers with very large instantaneous dynamic ranges. This is necessary to ensure target detectability when clutter conditions are severe; clutter-to-noise ratios (CNRs) in excess of 80 dB are often the case. Advanced radars with instantaneous dynamic ranges exceeding 90 dB are currently under development. However, a bottleneck still exists in the limited dynamic ranges of current state-of-the-art analog-to-digital converters (ADCs), which typically have about 30 dB less dynamic range than the receiver channels. [Ref. 22]

A technique to effectively increase dynamic range has been developed. Operating on the input signal prior to digitization, each radar return signal is predicted based on the previously returned signals. A replica waveform is generated and subtracted from the radar return signal prior to digitization. This technique allows the radar return signal to be digitized without distortion by a receiver with a wide instantaneous dynamic range even though it only uses a limited range ADC. After digitization, the full dynamic range of the radar signal is restored by adding the replica waveform to the ADC output. This can cost-effectively enhance the performance

17

of both civilian and military radars operated in severe ground clutter environments. [Ref. 22]

The technique is as follows; an algorithm predicts the radar return signal for pulse "n" using the radar return signals from previous pulses (n-1) to (n-p). The replica waveform generated by the prediction algorithm is then subtracted from the actual radar return signal, reducing the instantaneous dynamic range of the difference waveform entering the ADC. This subtraction reduces the dynamic range sufficiently to ensure saturation-free operation by the ADC when large clutter returns occur. It is not necessary for the replica waveform to exactly match the radar return signal; only that the voltage difference between the two waveforms falls within the dynamic range of the ADC. The reconstructed full radar return signal is recovered in the processor by adding a similarly processed replica waveform to the ADC output. The reconstructed return signal is then used for the radar return signal in the next pulse. The predictive filtering process is initialized by attenuating the first few radar signals and amplifying them after digitization. [Ref. 22]

This dynamic range enhancement technique relies on a strong pulse-to-pulse correlation of the radar return signals, which is the case in severe clutter environments. If non-correlated interference occurs (i.e., jamming), the receiver may have to resort to conventional techniques such as

18

sensitivity time control (STC) and automatic gain control (AGC) to avoid ADC saturation. [Ref. 22]

The viability of the dynamic range enhancement technique has already been demonstrated using both synthetic data and an E-3A AWACS radar. Tests involving the synthetic data show that a latency of one pulse repetition interval (PRI) reduces dynamic range by about 3.9 dB, 2 PRIs by 6.5 dB, 3 PRIs by 8.3 dB, and 4 PRIs by 10.0 dB. Additional improvement expressed in dB is nominally a linear function of the number of incorporated pulses. Over 30 dB of dynamic range enhancement has been achieved, thus meeting the needs of the previously mentioned receiver channels. Additionally, artifacts generated by the technique are sufficiently small so as not to cause excessive false alarms. [Ref. 22]

f. Analog/Digital Converters

ADCs define the boundary between a radar's analog and digital signals and, as such, are often the bottleneck on system performance. Typical ADC requirements are 10-12 bit resolution @ 100 MHz sample rates for high definition video and ultrasound imaging, 12-14 bit resolution @ 20-40 MHz for communication systems and signal analyzers and 7-8 bit resolution @ >1 GHz resolution in transient waveform digitizers. [Ref. 23]

Noise and aperture jitter are probably the biggest problems in ADCs. Clock signals are one of the major noise sources generated in the comparators. Internal noise

19

and spurious harmonics are generated by temperature fluxuations and nonlinearities. Internal and the theoretical quantization noise combine to form total noise, which restricts the effective signal-to-noise ratio (SNR). The effective maximum SNR for an ADC is equal to 6N + 1.76 dB, where N is the converter's number of bits. [Ref. 24]

Research shows that ADCs employing complimentary metal-oxide semiconductor integrated circuit (CMOS IC) and bipolar technology increasingly resemble one another in architecture, although they may employ different subcircuits. CMOS converters inevitably use closed-loop, auto-zeroed circuits in a precision analog signal path, while bipolar circuits, at least at the 10-bit level, may be open-loop and thus, capable of higher speed operation. ADCs implementing bipolar technology normally use 2-stage subranging. Passive circuits are also used in bipolar open-loop ADCs to interpolate the outputs of a coarse conversion and compensate for problems of differential nonlinearity. [Ref. 23]

Current state-of-the-art optical ADCs are capable of 14 bits @ 20 MHz [Ref. 25]. Research has also been published on high speed ADCs using integrated optical guided waves (IOGW). The technique employs Mach-Zehnder interferometers which preprocess the analog signals using symetrical residues directly from the antenna. This allows these ADCs to digitize signals at a higher resolution with a fewer number of comparators. Other advantages include a smaller number of interferometers. Thus, the required RF drive

20

power is reduced. Additionally, the interferometer lengths do not grow exponentially because the folding periods are closely spaced. This simplifies the design since identical folding circuits (interferometers) can be used. Finally, using symetrical residues, any combination of folding periods and comparator arrangements can be analyzed precisely. Resolution on the order of 11 bits with three interferometers and 39 comparators is possible. [Ref. 26]

The flash ADC has remained the most commonly used architecture for high speed A/D conversion for many years. It is the fastest and requires 2^N-1 comparators where N is the number of bits. In a flash ADC, the conversion rate is fundamentally limited by the decision time for comparing the input with the threshold levels. However, single-step flash converters resolving up to eight bits on a single chip are becoming practical. [Ref. 23]

A new signal level detector for a flash-type ADC has recently been introduced. Normally, as the clock frequency increases, so does the generated noise, creating an upper limit on the conversion speed. In this detector, the clock signal is omitted. Thus, there is no clock line to be distributed across the whole chip in the mask layout and clock feedthrough noise is not a problem. Using this flash ADC, a resolution of up to eight bits is feasible. [Ref. 27]

Sigma-Delta (SD) converters are capable of high resolution and are becoming increasingly important for relatively low bandwidth applications. They are widely

21

employed for their robustness with respect to component inaccuracies. Additionally, they are ideal for inexpensive on-chip VLSI implementation because they require fewer and simpler components than Nyquist rate (flash) converters; this is at the expense of using sampling rates many times faster than the Nyquist rate. [Ref. 28].

SD ADCs aren't as fast as flash converters because while they require only a single comparator, they take N clock cycles to complete a conversion. In SD modulation, the analog input is sampled at a very high frequency and the quantization error introduced by coarse quantization is spectrally shaped by feedback loops so that the quantization error falling into the signal baseband is highly attenuated. ADCs using SD modulation are able to deliver high-resolution performance from untrimmed analog circuitry using oversampling and noise shaping, but they require complex digital circuitry to suppress the out-of-baseband quantization error. [Ref. 29]

Above the ultimate limit set by the circuit noise (the flicker noise and thermal noise), SD ADC resolution is predominantly governed by three factors; [Ref. 29]

- the ratio of the modulator clock rate to the Nyquist rate (oversampling ratio)
- the order of the modulator,
- resolution of the internal quantizer.

The most feasible way to increase SD resolution is to increase either the modulator order or the internal quantizer resolution. Higher order modulators can be constructed using

either single or multistage configurations. Tradeoffs between these two concern input amplitude range, stability and component sensitivities. Higher order multistage modulators are more sensitive to component inaccuracies, but are more stable and have a wider input amplitude range compared with the same order single stage modulator. Internal quantizers can be either single or multibit. Multibit internal quantizers tend to be more stable than single bit ones. However, multibit advantages are balanced by strict accuracy requirements on the internal multibit DAC. Introduced errors, including nonlinearity, must be extremely small. [Ref. 29]

For lowpass signals, high resolution conversion requires the sampling frequency, f_s, to be much greater than the signal frequency which in this case, is also the signal bandwidth, f_o. [Ref. 30] For bandpass signals which may also be centered at high frequencies, bandpass SD modulation requires f_s to be much greater than the signal bandwidth, f_o, rather than the maximum signal frequency. Multiband sigma-delta (MBSD) (also known as subranging) ADCs can achieve a higher given f_o, f_s and analog modulator order for either lowpass or bandpass signals. Although the total unshaped noise power across the entire signal band is about the same, there is an improvement in resolution. Instead of comparing an analog input simultaneously with all possible quantization thresholds, it is first located within a coarse division of the full scale. Then, the input is compared to a finer division of the scale with different noise-shaping transfer

23

functions per subscale. While a given sample progresses to the next subscale, a new sample is acquired and applied to the preceding subscale. The process is recursively repeated until it is located to within accepted resolution. Then, each band is converted in parallel and a bank of finite impulse response (FIR) filters attenuates the out-of-band noise for each one. The overall throughput rate is determined by the time required for each subquantizer to produce a decision, which theoretically, may be as fast as a flash converter. The only cost of the higher resolution is the extra hardware needed for each band. [Ref. 30]

MBSD ADCs can achieve higher resolutions than current oversampled noise shaping converters for a given signal bandwidth, sampling frequency, and modulator order. For example, operating at 1.024 MHz and 64 KHz bandwidth with second order modulators, the architectures's resolution is four to five bits higher than that of a standard second order SD. This is very much the norm for eight or more bit quantization at high speed. [Ref. 23]

Currently being studied by researchers at Berkeley is a double loop SD modulator, which can be used by itself or as a building block in cascading modulators. For dynamic inputs, this double loop SD modulator is both stable and about two dB superior in both dynamic range and peak SNR to the best-known double loop SD modulator. [Ref. 28]

A new fourth order SD modulator created by a cascade of two second order stages has also been proposed

24

[Ref. 29]. A one-bit quantizer is used in the first stage and a multibit quantizer in the second. This modulator is tolerant of the DA multi-bit conversion error and therefore, can deliver a very high SNR in the baseband. Another significant advantage is the reduction in total noise output and thus, a reduced load on the following digital filter normally associated with multibit modulators. Finally, this new modulator has better stability performance because in each stage, only a second order noise shaping loop is employed. In practical implementation, the system's performance is limited mainly by mismatch between the SC circuits and the digital circuits. [Ref.6]

Integrated optical SD converters are also being investigated for wide bandwidth applications. The best models provide high resolution, direct digitization and are capable of converting 4 bits @ 1.2 GHz. Experimental models can convert 14 bits @ 1.2 GHz. [Ref. 25]

2. Signal Processors

There is an extensive amount of research regarding radar signal processing, especially in the specific areas of SAR (synthetic aperture radar), ISAR (inverse synthetic radar) and STP (space-time processing). There are several reasons for this, but the most basic one is that upgraded processing algorithms can be implemented into existing hardware relatively easily. Dr. Wolfgang Stehwien, a researcher at Litton Systems Canada Limited offers some observations on the

25

subject.   His comments are his own and do not necessarily reflect opinions held by Litton Systems Canada Limited's management.   According to Dr. Stehwien, "Implementation of new algorithms in production radar systems is very much a function of the market potential for any new system...   The market for new radars is limited by a number of factors:

1) They are expensive, requiring many millions of dollars in development funding, which few customers can afford.

2) The biggest customer to date, the military, is reducing its purchases and keeping its old equipment alive longer.

3) Offshore customers buy only a small number of systems at a time and export restrictions often prevent such sales altogether.

Making 'small' modifications to existing systems and squeezing more life out of them is considered safe, low-cost, and altogether tempting...   There have been few technological developments that naturally lead to new radar architectures, only 'refinements'...   Improvements in transmitter and processor technology provide only marginal increases in detection performance.   Customers generally know this and ask for more 'bells and whistles' such as fancy colour displays, avionics integration, etc., rather than plain radar performance.   This also naturally leads to add-ons, rather than an outright new development." [Ref. 31]

a. *SAR*

In conventional SAR, the signal data is collected with the antenna pointed perpendicular, or broadside, to the flight path of the platform aircraft or satellite. In squinted SAR, the antenna is pointed forward or aft of the broadside position by several degrees. This provides imaging of the earth's surface at different look angles. [Ref. 32]

While recent approaches to high squint SAR processing allow accurate focusing for points at a fixed slant range, their processing algorithms make approximations to the exact focusing operator. Thus, the variations in range of the secondary range compression (SRC) term in the focusing operator remains a problem. Increasing the squint angle increases the azimuth frequency and range dependance of SRC, causing noticeable degradation of the images produced by the range-Doppler algorithm. [Ref. 32]

A chirp-scaling technique has been presented which accommodates the range variance of SRC by modifying the phase modulation of the transmitted pulse. This algorithm incorporates an extra frequency domain filtering step, providing an alternative to the computationally demanding step of interpolation in range migration correction. In this simpler method, the phase modulation of the transmitted pulse is modified according to the squint angle while the chirp scaling accommodates the secondary range variance. [Ref. 32]

When chirp-scaling is applied, a range-varying frequency rate is induced which cancels the range variance of

27

the SRC term. Scaling is accomplished by multiplying the uncompressed range signal at each azimuth frequency by a phase function. Experimental results give fairly accurate focusing for squint angles up to nearly 30 degrees. [Ref. 32]

Another newer technique for processing highly squinted data also employs a chirp scaling approach, but with integrated motion compensation. This approach, extended chirp scaling (ECS), is a generalized algorithm suitable for the high resolution processing of most airborne SAR systems. ECS employs a modified chirp scaling algorithm to accommodate the correction of motion errors, as well as variations of the Doppler centroid in range and azimuth without using computationally-complex block processing. Experimentation shows that by introducing a cubic phase term in the chirp scaling process, once again, data acquired with a squint angle up to 30 degrees can be processed with no degradation. [Ref. 33]

The ECS experimental data start with a squint angle of 7.8 degrees and very strong motion errors, intentionally introduced by the pilot. A comparison of the results obtained by processing with the range-Doppler and hybrid algorithms show that no significant differences can be measured as far as the geometric and radiometric resolution of the images are concerned. The azimuth geometry from the different algorithms is also compared and the differences are less than one pixel spacing (measurement accuracy). [Ref. 33]

28

(1) Motion Compensation. Target motion can severely distort the image in a conventional SAR, causing targets with even small components of radial velocity to be lost or appear as position shifts proportional to the product of the range being imaged and the cross-track velocity, and inversely proportional to the platform velocity. By isolating the spectra of the moving targets and translating them to a point near the origin before carrying out conventional SAR processing, the moving targets can be made to appear at their correct locations in the final image. [Ref. 34]

A somewhat promising algorithm to locate moving targets at their correct positions contains the following general steps: 1) Transform a sequence of radar target returns to the frequency domain. 2) Locate the spectral bands adjacent to a frequency interval, $[-f_s, f_s]$, where f_s is a frequency threshold to distinguish a moving target from a stationary one. The proper threshold value of f_s depends on the range of the cell for which data are being processed. If no significant spectral contributions are found outside the interval, it means no moving target appeared in the processing interval. 3) Translate each outlying spectral band back to the origin. 4) At this point, there are two methods capable of completing the SAR processing. The first is to convert the spectrum by inverse Fourier transform. The maximum amplitude of the correlated output is taken as the target position. The second method involves direct processing of the signal in the frequency domain. This procedure uses

29

the relationship between a correlation function and its Fourier transform. 5) Convert the resulting signal back to the time domain and correlate with the reference function from the conventional SAR. The correlator output will show a pattern in which the maximum amplitude is very near the correct location of the target. [Ref. 34]

For multiple moving targets, the translation is repeated for each one, and the spectrum to be converted to the time domain is obtained by summing all the translated spectra together. A simulation program has been written such that a target with various values of V_x and V_y is initially placed 100 km from a radar platform which is moving at a constant altitude of 1000 m and velocity of 100 m/sec. Simulation results show that the largest distance error at $-30 < V_x < 30$ m/sec and $-30 < V_y < 30$ m/sec is 3.45 m. [Ref. 34]

While current reconstruction algorithms for spotlight-mode SAR assume that the relative motion between platform and scene is known exactly, this may not be the case. Another research paper involves estimation of target rotational speed from SAR projections. The approach starts by assuming a range of possible target rotation speeds. To estimate the actual speed, the image is reconstructed using several potential rotation speeds within the range. The correct reconstructed image has a somewhat blurred peak somewhere in the image. However, the sharper the peak, the smaller the variance. The correctly reconstructed image has the smallest variance. The parameter of the image with

30

minimum variance gives the estimated rotational speed. Simulation results show the average estimation error is <0.78%. For 99.33% of the cases, the estimation error is < 3%. In the worst case, the estimation error is still <6.68%. [Ref. 35]

Moving target detection capability in SAR imagery is vital, a lesson learned in The Gulf War. The most recent research into moving target SAR imaging involves STP and DPCA, [Ref. 36, 37]. These topics are important enough to warrant in-depth discussion elsewhere in this thesis.

(2) Real Time Analysis. The near real-time high speed Alaska SAR Processor (ASP) became operational at the University of Alaska in Fairbanks in 1992. It takes 10 Megasamples/sec and performs 3.9 billion operation/sec [Ref. 38], surveying a 100km wide path with along- and across-track resolutions of 30 and 26 m respectively [Ref. 39]. The ASP takes data at ~1/3 real time, performs a two-dimensional correlation with geometric corrections, and outputs high-resolution image data to a digital recorder. Processing SAR data is computationally intensive; while conventional processing takes from 10 minutes to 2.5 hours to process a 100 x 100 km scene, ASP can process the scene in one minute. [Ref. 38]

ASP's algorithm does three passes through the data. In the first pass, the hardware extracts the satellite PRF and noise measurements from the telemetry data.

31

In the second pass, the hardware Fourier transforms some of the data to determine whether the SNR of the input data is within acceptable limits. Pass two also determines Doppler parameters associated with the sample SAR data using an iterative technique. In the third pass, SAR data is actually processed into an image using results from the first two passes, which are stored in the processor memories. [Ref. 38]

Although it is specifically designed for the European Space agency (ESA) remote sensing satellite (ERS-1), the Japanese earth resources satellite (JERS-1), and the Canadian RADARSAT satellite, its architecture is sufficiently general to be used for other similar SAR applications. ASP produces high-resolution 8" x 8" negatives which may be enlarged to 20" x 20" pictures without significant loss in resolution. During the first week of operation, ASP produced over 600 SAR images and currently receives about 30 Gbytes of information for processing each day. [Ref. 38]

For actual _real_ time processing of SAR signals, a time domain architecture has been proposed which uses a correlator for processing range and azimuth data. To get a fine range resolution, a linear FM waveform of large bandwidth must be transmitted. The range resolution is then easily determined by the transmitted pulse duration. The coherently detected signal is processed by compressing it in both range and azimuth directions. In compressing the range correlated data in the azimuth direction, no explicit range migration correction is employed. In the azimuth direction,

32

the resolution is determined by processing the changes in the phase of the received carrier signal. These changes in the phase of the received carrier signal constitute the target azimuth phase history. A data reduction rate of 8 times is achieved in the presummer circuit. Using moderately high speed multipliers, this architecture enables real time processing of SEASAT-type imagery. [Ref. 40]

Another real-time SAR processing algorithm is called the subband algorithm. It is based on the theory of multirate filter banks and features two aspects; subband decomposition and fast convolution. Subband decomposition performs azimuth compression, resulting in subband images. Due to the strong time-frequency relation of the reference sequence, each subband image corresponds to a subband aperture. The time difference between the subband images is a measure for the phase error in that aperture. Whereas traditional fast convolution algorithms using overlap-add or overlap-discard techniques which increase the computational complexity, this one does not require them if sequence lengths are longer than the discrete Fourier transform (DFT) length. To improve azimuth resolution, a correction is required of the phase error caused by unpredicted aircraft motions. An autofocus-based algorithm does this with four steps:

1) Process the SAR image using the subband algorithm.

2) Search for a high contrast area in one subsampled subband image.

3) Construct subband images with a high sample frequency of

33

just the high-contrast area.

4) Determine the time difference between subband images. [Ref. 41]

This subband algorithm has been successfully tested on a SAR image containing a number of corner reflectors. The focused resolution is approximately 0.5 m, while unfocused resolution is 0.8 m. [Ref. 41]

(3) Autofocusing Algorithms. The subject of autofocus is a popular one in signal processing research. High resolution SAR imaging requires that the radar platform motion be known very accurately. It is unlikely that any SAR can fully meet it's ultimate utility without some means for automatic image focusing. In particular, any constant error in the measured along-track velocity or the cross-track acceleration leads to a phase error that varies quadratically over the synthetic aperture. The process of estimating this quadratic phase error directly from the radar data is termed autofocus. [Ref. 42]

The fast autofocus algorithm presented here is called the shift and correlate (SAC) algorithm because its basic operations are a frequency shift followed by cross-correlation. The Doppler history associated with a point target is a linearly frequency modulated signal. The derivative of the instantaneous frequency, the Doppler rate, is proportional to the square of the along-track velocity.

Thus, an estimate of this along-track velocity can be obtained from an estimate of the Doppler rate. [Ref. 42]

The SAC algorithm forms two looks by bandpass filtering the Doppler signal. One look is frequency shifted and cross correlated by the other look. This time reversed complex conjugate of the first look serves as a matched filter. Cross correlation leads to a pulse compression after which the desired Doppler rate is obtained from the position of the resulting peak and the frequency shift. The looks are not focused and detected prior to the cross-correlation, so although a look correlation is also involved in the map drift algorithm, the two algorithms are fundamentally different. Also, unlike the map drift, the SAC algorithm is a single pass algorithm, calling for 50 times fewer arithmetic operations. [Ref. 42]

Tests using Danish airborne SAR images of both urban and agricultural scenes are presented in Table 2. The SAC algorithm and map drift algorithm velocity estimates are obtained from adjacent subscenes covering the entire scenes. Each subscene size is 2048 pixels in azimuth and 512 in range. The table compares the standard deviation of these estimates with the velocity accuracy, ρ_v needed to achieve a quadratic phase error of less than $\pi/4$. [Ref. 42]

Scene	Urban	Agricultural
SAC std.	0.47 m/sec	0.63 m/sec
Map drift std.	0.37 m/sec	0.73 m/sec
ρ_v	0.68 m/sec	0.80 m/sec

Table 2; Accuracy of Autofocus Algorithms [Ref. 42]

The most recent research on autofocus presents a refined implementation of Phase Gradient Autofocus (PGA) for phase error correction of spotlight mode SAR imagery. Since its initial publication in 1988, this algorithm enjoys widespread use throughout the SAR community. Based on optimal estimation theory and many real world SAR systems, PGA is exceedingly robust over a wide range of applications and provides near diffraction-limited resolution on virtually any phase degraded SAR image. Bright isolated point-like reflections are not needed. Therefore, scenes completely devoid of cultural features can be restored. Defocused SAR images can be restored to their designed quality in nearly all instances. Also, PGA can be implemented so as to require a fixed amount of data and calculations, which become a smaller and smaller fraction of the computational load for large image formation problems. Thus, its computational load does not correlate to image size as do other autofocus methods. [Ref. 43]

In PGA, there are four processing steps; 1) center shifting, 2) windowing, 3) phase gradient estimation, and 4) iterative correction. The purpose of center shifting

is to select for each range bin, n, the strongest scatterer and shift it to the origin (center of the image). This removes the frequency offset due to the Doppler of the scatterer. The operation aligns strong scatterers and subsequently improves the SNR for phase estimation. It also aligns regions undergoing subtle contrast changes. Windowing preserves the width of the dominant blur for each range bin while discarding data that cannot contribute to the phase error estimate. Progressively decreasing window width works quite well; the initial width is selected to span the maximum possible blur width, and is progressively narrowed by 20% in each iteration. In the iterative phase, the estimated phase gradient is integrated and any bias or linear trend is removed prior to correction. As the image becomes more focused, individual scatterers become more compact, the signal to clutter improves, the center shifting more precisely removes the Doppler offsets, and the algorithm is driven toward convergence. When the root mean square error drops to a few tenths of a radian, the image is well focused and does not improve with additional iterations. [Ref. 43]

Published research shows that features corresponding to ship or periscope wakes can sometimes be seen in SAR images of ocean scenes such as those from SEASAT. These features appear as bright or dark lines that may trail for several kilometers. An automatic detection scheme for ship-generated wakes has been devised. SEASAT images are initially thresholded to remove all the excessively bright and

37

dark pixels. These pixels are likely to be returns from a ship. The removal is determined by comparing the pixels to predetermined thresholds. Next, a mean high-pass running filter reduces the effects of slow spatial variations in the image. Following filtering, a radon transformation which maps lines in the filtered image is applied. Strong linear features transform into positive peaks. [Ref. 44]

The algorithm is based on two exclusive hypotheses:

1) the image contains a wake feature.

2) The image contains no wake feature(s).

A Wiener filter-based shape detector is then applied to the significant peaks and a "gain value" is calculate for each peak. The gain value is essentially a measure of how closely the peak's shape matches the expected shape for a proper wake feature. If a positive (bright) peak is being considered:

$V=G-1.25$

And for a negative (dark) peak:

$V=G-1$

Where G is the gain value. These parameters were deduced from actual SEASAT data. Next, probabilities are calculated:

$P(UNCERTAINTY)=0.5(1-\tanh(V))$

$P(WAKE)=(1-P(UNCERTAINTY))\tanh(A(N-B))/2$

$P(NON-WAKE\ FEATURE)=1-P(UNCERT.)-P(WAKE)$

where N is the number of intersections of relevant lines which form the peaks and A and B are constants based on ship wake data. If an image contains both wake and non-wake features,

38

The algorithm will give a high wake probability and low non-wake probability.   Also, some variations in the initial probabilities are likely when different ocean locations are examined.   For example, there is less chance of observing a ship's wake outside shipping lanes than within.   Results for a library of 37 SEASAT images show no false alarms and only one undetected wake. [Ref. 44]

Conflicting research has been published regarding the use of autofocus in wave and ship wake detection, as illustrated in [Ref. 45].   The most recent (1994) article on the topic [Ref. 46] seems to successfully summarize and resolve the focusing mechanism controversy.   It begins with a 1978 report which indicates that airborne SAR images of the ocean surface waves propagating in and near the azimuth direction can be enhanced by defocusing the processor. The optimum defocus corresponds to approximately half the azimuth component of the wave phase velocity.   However, image enhancement by defocus is not possible if waves are propagating -exactly- in the range direction, since there is a singularity and a defocus of infinite amount would be required. [Ref. 46]

This report goes on to explain why applying a processor defocus will generally yield an enhanced image, why the same defocus applies to both image modulations brought about by the radar cross section and by the velocity bunching process, and why the effects apply to both single look and multi-look systems independently of look relocation.   Two

39

interpretations are given for the case when surface scatterers are stationary, but modulated in reflectivity by a propagating wavefield. [Ref. 46]

The first autofocus interpretation is called the degrade-and-shift model. In it, a processor focal adjustment apparently degrades, but at the same time, displaces the point image. However, the overall image can be enhanced because an appropriate defocus results in shifting of points in such a way that the image can most closely resemble the image of the time-invariant (frozen) reflectivity distribution, and thus yield an enhanced image. Degrade and shift is very useful for insight, but clear and unambiguous predictions are difficult. [Ref. 46]

The second autofocus interpretation is the defocus-and-refocus model. The image is genuinely defocused and then refocused by adjusting the processor focal setting, yielding an enhanced image. This model considers the effective impulse response and provides much clearer predictions. [Ref. 46]

In justifying the second interpretation, it is shown that the radar return from stationary scatterers of time-varying reflectivities is identical to that from physically moving scatterers of constant reflectivity. Thus, the theories are not contradictory, they are equivalent. Additionally, the same defocusing effect applies to image modulations brought about by the velocity bunching process. In conclusion, while the two different interpretations are

logical consequences of SAR imagery of time-varying scatterer reflectivity, the authors recommend the use of a processor defocus to enhance the image of half the wave phase velocity. [Ref. 46]

b. ISAR

ISAR images are produced by radar range/Doppler measurements of a rotating object. Due to the larger length of radar waves, the image resolution is much poorer than photographs. In order to classify objects, powerful segmentation techniques are required.

It is possible to store many of the geometrically possible ISAR images of complex targets and use them for automatic target recognition (ATR) of surface ships. The problem involves efficiently organizing a database which contains a huge number of ISAR returns. The goal is to economize memory volume while minimizing search time. An effective algorithm has been developed to do this. It employs a multi-resolution wavelet representation working with a hierarchical Tree Structured Vector Quantizer (TSVQ) in a clustering mode. Wavelet representations of return signals allow break down using superposition of the signals in terms of different structures occurring at different times. This leads to positive identification of the various targets in the database. [Ref. 47]

In the received ISAR data, dominate scatterers typically have highly directive returns with small variations

41

in aspect. Additionally, varying the radar pulsewidth changes the resolution of the returned pulse. Thus, small changes in the aspect elevation and pulsewidth produce large variations in the returned signal. These radar returns are separated and clustered based on their dominant features and compared with a tree-shaped hierarchical organization of radar data starting with the dominant returns first. Next, sophisticated versions of vector quantization (VQ) are used to further compress and cluster the high resolution wavelet representations, further streamlining the target identification process. The advantage from increased resolution is the availability of more detailed information, and ultimately of specific features, characteristic of the radar return from a specific target ship. [Ref. 47]

Experiments indicate the combined algorithm results in orders of magnitude faster data search time with negligible performance degradation from the full search vector quantization. The combined wavelet-TSVQ algorithm has been compared with other VQ algorithms based on the finest resolution possible by plotting total distortion compared to the number of resolution cells. In all experiments, the results are quite similar. Performance curves show the combined algorithm is very robust with respect to wavelet selection. Its performance sensitivity is also examined. The tree itself is sensitive to the wavelet used, but the algorithm's performance is not. Overall, the combined algorithm provides an efficient indexing scheme using

42

variations in aspect, elevation and pulsewidth to develop ATR surveillance and potentially, fused multi-sensor systems. [Ref. 47]

Another ISAR-based ATR development uses signal processing employing a hybrid neural network architecture. It contains a feature map for cluster segmentation and a cascaded combination of an unsupervised and supervised trained neural networks for the classification. The unsupervised trained self-organizing feature is used for object segmentation, followed by the supervised trained multi-layer preceptor which classifies the segmented objects. The classifier's decision is fed back to the adaptive segmenter to reinforce the classification results. This is a direct contrast with conventional feedforward classification systems. [Ref. 48]

Neural network-based ATRs are another ongoing research area for both military and commercial applications. In the study reported here, "hopeful" results were obtained using data from the Naval Research Lab (NRL) digital simulation model. [Ref. 48] Still, it is interesting that neural network ATRs are specified by Rockwell in their Radiant Outlaw/LIDAR system [Ref. 49].

c. *Space Time Processing*

In an airborne look-down radar, target signals often have to compete with strong ground clutter returns. Additionally, platform motion causes a significant Doppler spread of the clutter, depending on frequency, squint angle,

43

sidelobe levels and platform velocity, as shown in Figure 1. [Ref. 50]. Practical airborne antennas, with relatively large sidelobes, may be subjected to large sidelobe clutter which will mask moving mainbeam targets at the same Doppler frequency. No degree of resolution can distinguish the target from clutter. [Ref. 50]

$$f_d = \frac{2Vf_0}{C} \sin \varphi_0 \qquad f_d = 0 \qquad \varphi_0$$

$$f_d = \frac{-2Vf_0}{C} \qquad f_d = +\frac{2Vf_0}{C}$$

Clutter Power Spectrum

$$-\frac{2Vf_0}{C} \qquad 0 \qquad \frac{2Vf_0}{C} \sin \varphi_0 \qquad +\frac{2Vf_0}{C} \qquad f_D$$
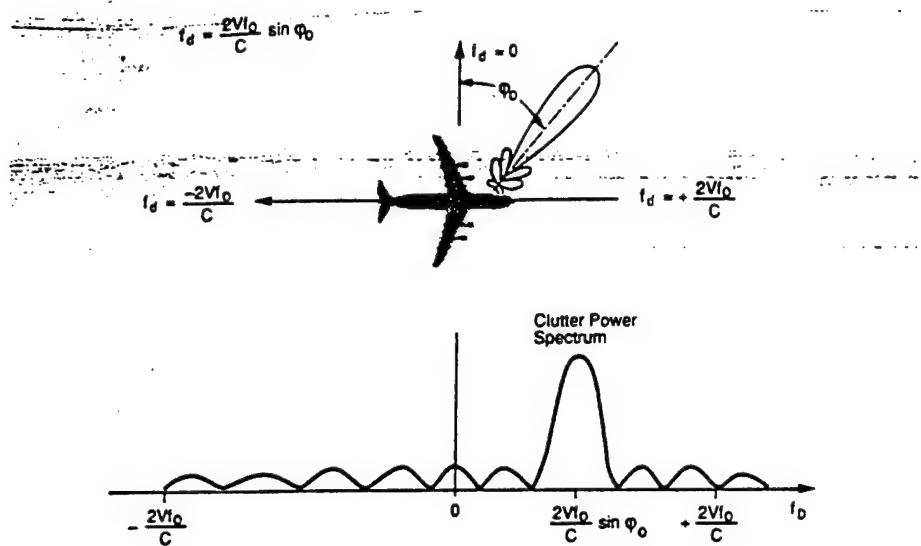
Figure 1; Doppler Spectrum of Received Clutter
for Airborne Radar [Ref. 51]

The conventional cure for excess clutter is to reduce sidelobe level, but for small cross-section targets this may not be practically achievable [Ref. 52]. A conventional moving target indicator (MTI) radar is ineffectual in cancelling airborne clutter because it only uses temporal (time) degrees of freedom. Since there is an interdependent clutter Doppler and clutter angular location, significantly better performance can be achieved with two-

dimensional filters using both spatial and temporal frequency characteristics to discriminate targets from clutter [Ref. 53]. This two-dimensional filtering approach is generically referred to as STP. Nulls are adaptively placed on the undesirable clutter and jammers and the airborne STP radars can adaptively detect small targets in their presence, provided the covariance matrix of the interface is available. [Ref. 52]

The optimum STP has array weights based on a covariance matrix. However, a direct implementation of the matrix is not possible. This is because of poor numerical stability in the inversion of the interference covariance matrix when large dynamic range signals are experienced [Ref. 54]. Another difficulty in estimating the covariance matrix is the need to obtain a sufficient number of independent samples. This is overcome by combining subaperture averaging, or "spatial smoothing" of the received data with conventional range bin averaging. [Ref. 52]

The simplest system to combine both spatial and temporal degrees of freedom is the displaced phase center antenna (DPCA)[Ref. 51]. It was developed for range unambiguous clutter, but modification allows for cancellation of range ambiguous clutter in both main and sidelobes of the antenna's far field. This is accomplished by direct compensation for the platform motion.

The problem with nonadaptive DPCA is it's sensitivity to antenna leading and trailing antenna responses and platform velocity knowledge [Ref. 53]. Internal clutter motion, crabbing (flying "sideways" to compensate for crosswinds), and scattering from near-field obstacles can also limit STP effectiveness. Internal clutter motion smears the clutter linearly, producing severe distortion in the radiation pattern. Aircraft crabbing produces the same effects as internal clutter motion, but crabbing smears the clutter in a curve. An increase in the number of processed pulses cures both of these clutter problems. Near-field obstacles tend to spread the clutter over the entire sine-azimuth Doppler plane. The processor attempts to place a spatial null on each near-field obstacle. A series of depressions is produced because it is trying to cancel all the clutter and simply doesn't have enough degrees of freedom to do that. Increasing the number of array elements is quite effective in cancelling the near-field effects because it allows a deeper null to be placed on each obstacle. The last limit to STP effectiveness is "channel mismatch", wherein each receiver channel has a different variation of the phase and amplitude errors across the frequency band. This produces a spatial ripple across the received wavefront that differs from the expected planar wavefront within the steering vector. A single receiver weight can't possibly cancel clutter across the entire bandwidth. Channel mismatch is minimized by controlling the

dispersive errors and increasing the number of receiver elements. [Ref. 51]

With the above mentioned limitations under control, it is possible for STP-based airborne surveillance radar to achieve improved detection of small airborne targets in severe clutter, especially compared to low-sidelobe beamforming or DPCA systems. Current research efforts focus on the areas of calibrated clutter measurements, real-time processing hardware development, and theoretical performance evaluation of competing STP architectures. [Ref. 55]

In the evaluation of performance measures, two STP approaches delivering the same signal-to-noise ratio (SNR) may exhibit dramatically different constant false alarm rate (CFAR) performance. Therefore, spatial processor performance is more objectively measured by the CFAR, not SNR [Ref. 55]. Consider the SMI, the modified SMI, and the generalized likelihood ratio (GLR). Processing can be applied with a variety of adaptive algorithms to any of these three algorithms and all have similar SNRs. However, only the modified SMI and GLR have CFAR in Gaussian clutter and only the GLR is robust in non-Gaussian clutter. [Ref. 56]

In 1992 and 1994, A number of suboptimal space-time processing techniques were considered; factored processing (FA), extended factored processing (EFA), and joint-domain likelihood (JDL), each of which employs the GLR detection algorithm. [Ref. 50, 55]

47

The most popular is the FA [Ref. 50]. FA is a suboptimal solution to reduce ground clutter in an airborne radar system. Doppler filtering is performed on each spatially sampled element first, followed by spatial filtering in each separate Doppler channel. This separation or "factoring" of the temporal and spatial filtering functions leads to considerable computational savings (compared to that required in fully adaptive processing) at the expense of a slight performance loss [Ref. 50]. FA is motivated by the fact that it is much easier to achieve the low sidelobe feature in the Doppler domain than the spatial domain. However, the low sidelobe comes with a wider mainlobe, resulting in a loss of Doppler resolution. [Ref. 55]

The basic idea behind EFA is to include a fixed number of adjacent bin non-zero correlation values in the weight formulation. These weights are applied to an architecture using less than fully adapted processing. Performance improves greatly for relatively small increase in computational complexity [Ref. 50]. EFA can avoid the main problem of the FA via Doppler beam sharpening since the clutter components on adjacent Doppler bins are highly correlated. Unfortunately, it is difficult to analyze the tradeoff between the adaptation loss and the degree of freedom loss with this approach. [Ref. 55]

The 1992 flight test results show a peak clutter of 56 dB. Second order system processor performance is better than first order in both simulated and flight experiments.

Moreover, the second order clutter-to-noise ratio is 5-7 dB better than the fully adapted SNR value [Ref. 50]. Figure 2 gives a graphical comparison of the JDL, FA, and EFA techniques.
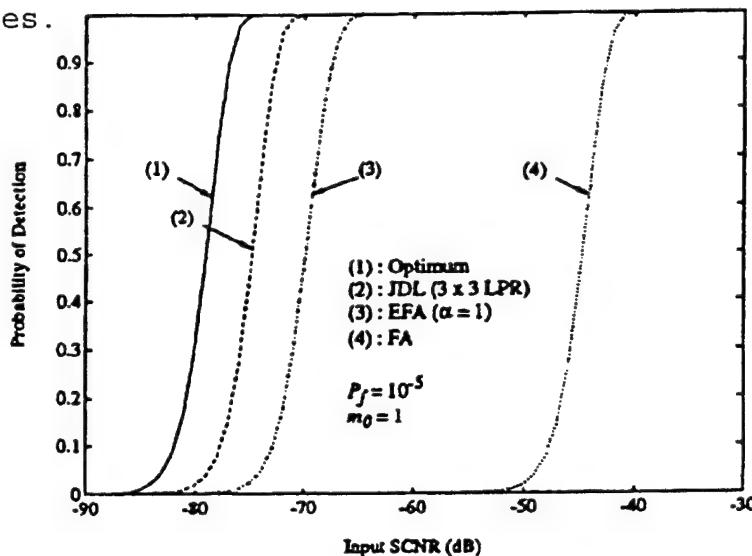
Figure 2; Detection Performance Comparison as a
Function of Input SNR. [Ref. 55]

Another comparison of adaptive STP architecture pits a JDL algorithm against two variations of FA; a cascaded space-time algorithm, and a cascaded time-space algorithm [Ref. 57]. The JDL architecture has spatial degrees of freedom derived from the N element-level channels. Time domain degrees of freedom are derived from an M-pulse coherent processing interval. The JDL architecture produces a set of NM complex weights, one for each tap on each spatial channel. The JDL processing approach is a "fully transformed domain" processing approach or more simply put, the whole set of data is processed all together by an optimum weight matrix [Ref. 56].

49

The Space-time cascaded architecture uses an "adapt-then-filter" approach. The spatial optimum weight vector is first operated on each snapshot in the spatial domain. Then the output of the spatial processors is further processed in the temporal domain [Ref. 56]. It is essentially an M-pulse JDL STP prior to Doppler filtering. The covariance matrix has dimensions NM x NM [Ref. 57].

The Time-space cascaded architecture implements Doppler filtering through a fast Fourier transform (FFT) filter bank prior to adaptive weight calculation. This is known as "filter-then-adapt". The Doppler filters' outputs are sampled to form an estimate of the covariance matrix. This matrix is used to calculate the weights to be applied to the input data. [Ref. 57]

Cascade processing, especially the space-time configuration, has been so popular in recent years that it seems to replace the JDL in airborne surveillance applications. However, the most recent research indicates neither of the two cascade configurations is theoretically better than the other. In fact, the performance potential of both cascade configurations falls well below that of the JDL processor, especially in more nonhomogeneous clutter [Ref. 56]. Additionally, a cascade implementation of separately designed STP and CFAR algorithms will not always maintain the desired CFAR feature and neither of the two cascade configurations make full use of the signal-clutter separation which must be considered to deal with clutter having both

50

angle and Doppler (non-homogeneous) spectral spread [Ref. 55].
Finally, the two cascade configurations have practical
limitations involving loss of angle or Doppler resolution
[Ref. 56].

Another 1994 research paper compares the
detection performance potentials of the two cascade
configurations and the JDL configuration under the assumption
that the clutter/interference plus noise covariance matrix is
known. The new algorithm presented is the JDL-GLR. It
approaches actual optimum JDL performance by separately
processing grouped adjacent angle-Doppler bins. [Ref. 56]

Figure 3 shows five processors;

1) the JDL
2) the JDL-GLR with seven localized processors
3) the time-space (TS) configuration
4) the space-time (ST) configuration
5) an optimal conventional beamformer (e.g., MTI)
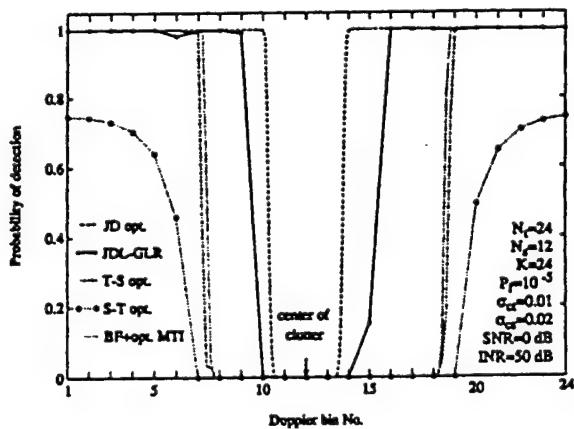
Figure 3; Processor Detection Performance Comparison [Ref. 56]

51

In Figure 3, the JDL-GLR is the only one that approaches the joint domain optimal performance, except at a few bins adjacent to the center of the strongest clutter spectrum component. Additionally, as the number of channels increases, the JDL-GLR offers a computational load reduction. Finally, the JDL-GLR can further reduce the computational load by deleting the localized GLR processors in the region where detection performance improvement is unnecessary. [Ref. 56]

Some of the most recently published STP research investigates its limitations in the electronic warfare environment. A major concern is terrain bounce jamming. This occurs when a jammer's transmitted energy covers the same surface as the down-looking radar footprint. The jamming signal can easily enter the high gain radar mainbeam and provide a significant source of interference. Whereas current generation STP architecture is unable to cancel this interference, future radar architecture must carefully consider both current and potential threats. [Ref. 58]

3. Exciters

At Westinghouse, Doppler processing research shows advances in the fields of exciter master oscillator, waveform generation and miniature atomic clock technology. It is crucial that the exciter provides multiple frequencies and waveforms with improved spectral purity and signal frequency stability for the transmitter and receiver local oscillator signals. These low noise exciter signal spectral

52

characteristics are dependant on several important master oscillator resonator parameters. They include: (1) high loaded Q, (2) frequency stability, (3) high drive level capability and (4) low vibration sensitivity. [Ref. 59]

The High overtone Bulk Acoustic Resonator (HBAR) exhibits a very high Q and a high (UHF) operating frequency range. It has been under development for several years. Thin sputtered ZnO film transducers and metal electrodes are deposited on opposite sides of a highly polished low acoustic loss crystal. Thus, the crystal itself need not be piezoelectric. This allows use of materials with resonant Q values an order of magnitude higher than quartz. Most of the recent HBARs use longitudinal wave propagation in yttrium aluminum garnet ("YAG") crystals, operating in the 300-700 MHz range, resulting in HBAR frequency control to 1 ppm frequency accuracy. An additional improvement in HBAR frequency stability is demonstrated using an increased thickness (resulting in a 700 nsec. delay) HBAR crystal. The one potential problem with the YAG HBAR is its linear -30 ppm/°C temperature coefficient. However, as a temperature-stable alternative to the YAG HBAR, other types of high Q, non-quartz, piezoelectric crystals, such as $LiTaO_3$ resonators, are being investigated. These exhibit frequency stability noise levels 10 to 13 dB higher than YAG HBAR, but are still comparable to the "ultra-low noise" quartz surface acoustic wave (SAW) resonators. [Ref. 59]

53

The choice of a waveform generation techniques usually represents a tradeoff among a variety of factors including waveform fidelity requirements, spurious signal content and phase noise. For a multimode radar there is an additional requirement of multiple waveform generation. The best waveform generation technique is one in which each shape is produced using the same equipment. A digital waveform generator approach is a step in this direction.

Direct digital synthesis (DDS) techniques, such as those used in communication systems, are also valuable in radar waveform generation. DDS waveform generators possess several advantages over analog models, including multiple waveform capability with the same generator, fine resolution of waveform parameters, precise phase switching (+/- 0.006 degrees), low phase noise and insensitivity to vibration [Ref. 11]. The disadvantage of DDS is the spurious signal content as a result of quantization errors, distortion in the DAC or sampled signal alliasing effects. DDS also constitutes a source of additive clock noise. This additive noise is very low for silicon bipolar DDS waveform generators (<-145 dBc/Hz @ 1 KHz) but much higher for GaAs (<-125 dBc/Hz @ 1 KHz). [Ref. 59]

There are two ways to use the analog output from the DDS. An In-phase/Quadrature (I/Q) modulator can be driven by the DDS in which case, the DDS provides the modulation. Alternatively, the DDS can generate the carrier signal with modulation (the IF technique). The I/Q technique is easy to

implement for both new or existing designs. It also provides the widest bandwidth for a given clock frequency since the Nyquist criterion only applies to the modulation bandwidth. Its disadvantage is the poor image and carrier suppression (20-30 dB) of I/Q mixers which limit their signal fidelity. The IF technique uses the upper or lower sideband of a double balanced mixer so that mixer image, local oscillator, and intermodulation spurious signals can be filtered. This allows better signal fidelity at the expense of increased clock rates for the DDS as well as the need for a frequency plan in the exciter which can accommodate the waveform generator output frequency. [Ref. 59]

DDS is very effective in narrowband radar applications. The DAC clock rate in these systems is typically 50-80 MHz. The spurious-free dynamic range is about 70-80 dB. The discrete spurious in the spectrum are due to mixer intermodulation products, indicating that spurious associated with the DAC and digital circuits are below -80 dBc. [Ref. 59]

Improvements in wideband (100 MHz to 1 GHz) linear FM waveform generation techniques have also been made. A custom GaAs ASIC exists wherein a sampled digital waveform is produced and subsequently converted into an analog signal by a DAC followed by a low pass filter. The ASIC and DAC clock rates are 600 MHz and useful waveform bandwidths at X-Band are on the order of 600 MHz. This compares favorably with the

55

best DACs today which have 70-80 dB spurious noise performance at 20-50 MHz clock rates. [Ref. 59]

The final area of exciter research involves miniature atomic clock technology using rubidium as the working medium. Though less stable than conventional cesium beam tube clocks, rubidium atomic clocks offer the critical advantage of significantly smaller size. "Miniature militarized" versions typically have volumes of about 500 cm^3. Another development is an innovative atomic clock using a miniature, diode laser-pumped, cesium gas cell. It employs custom integrated circuit for most of the signal processing and control hardware. The company's goal is production of an efficient atomic clock occupying a volume of about 10 to 100 cm^3. [Ref. 59]

4. Antennas

Recent antenna research focuses almost exclusively on active-element, electronically-scanned, phased-array (AESA) antennas, which offer many substantial improvements over conventional mechanically scanned antennas. AESAs are composed of numerous individually radiating T/R modules whose composite beam can be shaped and spatially directed in microseconds, enabling simultaneous multiple target tracking. This is accomplished electronically by RF phase shifters associated with each individual radiating element. No moving parts are required. Independent control of output power, phase and receiver gain of each T/R module in the array allows for almost unlimited flexibility to choose beam shapes

56

optimized for mission applications. It also allows the transmit and receive apertures to be weighted and optimized separately for peak performance. The beam agility and inertialess scan provide for increased target update rates and overlapping modes, producing multi-mission capability. Additionally, AESAs have wider bandwidths (up to ~30%), lower sidelobes, and allow conformal installation on aircraft fuselages and ship superstructures. [Ref. 4]

An AESA radar's reliability is superior to mechanically scanned arrays by nearly an order of magnitude. This is due to the highly dependable T/R modules (200,000 hours MTBF) and the graceful degradation failure mode. Typically, greater than 5% or more module failures can be tolerated while maintaining acceptable performance as a multimode radar. [Ref. 4]

Relative value is a major concern in antenna design. Several studies agree that the unit cost of a T/R module must be ~$500 to achieve acquisition costs comparable to conventional radar antennas. Life cycle costs are already shown to be significantly lower. [Ref. 4]

Because of their compact, inexpensive design, PIN diodes were used as phase shifters in the 70's. However, no way has been found to avoid their high insertion losses. Ferrite phase shifters have since gained popularity as their initial size, speed and cost limitations have been overcome. [Ref. 60]

57

One very successful application of ferrite phase shifters is the Joint STARS phased array radar system. [Ref. 61] Two such equipped E-8A (Boeing 707) aircraft were instrumental in the Persian Gulf War, performing long range around-the-clock battlefield surveillance from a safe distance behind front lines. Their aperture is a planar, X-Band slotted array, 24' wide by 2' high, with a rectilinear grid of 456 by 28 horizontally polarized slots. Ferrite shifters scan the beam +/- 60 degrees in azimuth. Incoming wave direction is determined by measuring the received phases of the three one-third aperture interferometer antennas spaced eight feet apart. The arrays' manufacturer, Westinghouse Norden, expects to adapt the Joint STARS technology to smaller antennas, compensating for the resulting wider beamwidths with an imaging enhancement focusing technique and using software to remove phase errors. Other planned upgrades include implementation of a monolithic electronic ferrite phase shifter driver configuration. This increases the dual shifters' MTBF from 60,000 to 250,000 hours, improving the antenna assembly's overall reliability by 60%. [Ref. 61]

AESA antenna faults, their detection and correction are frequent research subjects. One such fault is structural deformation such as antenna bowing, which can be produced by G-load deflections or temperature gradients. Bowing can cause mainbeam broadening as well as errors in antenna beam pointing and interferomic angle measurements. [Ref. 62]

Experimental data show that random element failures tend to increase the array's average sidelobe level while contiguous element failures lead to degradation of the peak sidelobe level. While an array with failed elements at its ends tends to increase in beamwidth, an array with failed elements at the center tends to produce a narrower beamwidth. Regardless of the failed element location, the peak sidelobe level may rise from -33 dB to -23 dB and the average sidelobe may increase by more than 15 dB. [Ref. 62]

In an effort to maintain low sidelobe characteristics, a fault correction technique for AESA antennas can reshape the beam pattern of a partially failed array. Embedded in the array is a transmission line signal injector which transmits signals for monitoring the RF performance of each element. A failed element is sensed and eliminated after which a "sector nulling" fault correction algorithm is applied to the remaining elements. It compensates for the failed element by adjusting the complex weights of the remaining ones so the average sidelobe level is about 7 to 8 dB lower than without the nulling. [Ref. 63]

Another factor which limits AESA radar performance is the impact of the aircraft itself in the nearfield of an airborne antenna. Fuselage interference can increase the sidelobe size, thereby raising the level of the received clutter and jamming signals beyond the capability of an adaptive sidelobe canceler. This phenomenon may also influence shipborne and mobile ground antennas. [Ref. 64]

59

It is difficult to evaluate degraded antenna performance using just the affected pattern. Computer modelling, however, allows performance/position tradeoff studies to avoid blockage and diffraction caused by platform structures. Research shows the cost effectiveness of this approach is dependant on validating the code accuracy, especially for performance predictions of sidelobes below -45 dB. [Ref. 64]

The most intriguing antenna research involves FOPAIR (Focused Phased Array Imaging Radar). Whereas conventional antennas are usually designed to resolve targets in the far-field and are said to be unfocused or "focused to infinity", FOPAIR is designed for nearby remote-sensing applications, providing high resolution, pulse-compressed X-Band (10 GHz) images of the adjacent ocean surface at a rate of up to 180 frames/sec. It is designed for short range surveillance applications (50-400 m) from a fixed platform such as a pier or tower. [Ref. 65]

FOPAIR employs a single pyramidal horn and fast sequentially sampled antenna array. It uses a software-based beam-forming technique to generate high-resolution imagery without the need for multiple receivers or beamforming hardware. The array consists of 128 linear tapered slot antennas. These low-cost endfire antennas are easily fabricated on a printed circuit board. The elements are vertically polarized and are fairly directional with beamwidths of 18 and 24 degrees in the E- and H-planes,

60

respectively. A single receiver services the array via a 128:1 switching network. This substantially reduces costs. The receiver outputs are baseband I and Q channels each with a video bandwidth of up to 100 MHz. [Ref. 62]

During July, 1993, FOPAIR was deployed on the research pier at the Scripts Institute of Oceanography in La Jolla, Ca. Results that show worst case range migration effects are no more than one half-range cell. At a nominal range of 200 m, an azimuthal footprint of 80 pixels spans 70 m. The sampler is operated at 100 MHz, providing range resolution of 1.5 m. Once a sequence of complex images is captured, radial velocity and MTI images are generated. Radial velocity images are derived using the covariance or "pulse-pair" technique and MTI images are derived from frame-to-frame differences. [Ref. 65]

Although FOPAIR is designed for imaging areas much smaller than most SAR applications, it does share SAR's sequentially sampled array approach. Since only one aperture is available for processing, FOPAIR's azimuth resolution limit is range dependant. Also, it must implement multiple beams over a range of look angles to achieve spatial coverage. The resulting image is polar formatted. [Ref. 65]

Identification Friend or Foe (IFF) systems are often incorporated into search antennas to allow interrogation of radar contacts. The issue of inadequate IFF is one that resurfaced during The Gulf War. The biggest technical problem is determining whether the lack of response from a contact means it is hostile or it is friendly but with a non-operating

transponder [Ref. 66]. In Europe, the New Generation IFF (NG IFF), or EURONIS, is scheduled to enter full scale development this year. In the U.S., development has been place on hold, due to financial considerations and the disagreement over division of responsibilities between the U.S. Army and Navy. [Ref. 67]

5. Interconnections

Active phased array radars are critically dependant on the availability of many highly reliable microwave T/R modules. The multiplicity of connections is perceived as a weak point of the system and as such, connector capacity and reliability is a concern. In 1991, a fiber optic cable replacement to eliminate electromagnetic interference (EMI) in airborne radar unit-to-unit digital cables was designed, built and successfully demonstrated. The replaced cable connects several units within a radar system. It consists of 44 twisted shielded-pair heavy copper lines (88 individual wires) containing 26 high speed ADC lines and a maximum effective data rate of 58 MHz. The copper wires are susceptible to EMI and their connectors take up a large area on the inputs and outputs of the radar units. [Ref. 68]

The replacement cable consists of seven fiber optic links. Each contains a laser transmitter, fiber cable with connectors, photodiode detector and associated input and output electronics. One of the seven links transmits a 524 MHz high speed clock and another carries an output data

alignment signal. The remaining five links carry the sampled digital data. For simplicity, the replacement cable is designed so that all inputs are sampled at 58 MHz. A successful demonstration shows a composite data rate of 3.5 GHz. The noise figure dropped by 50 dB. Additionally, a significant weight reduction (110 lbs./100' reduced to 3 lbs./100') and size reduction (1" reduced to .25" diameter) are shown, although no specific attempt was made to do so. These reductions are graphically demonstrated in Figure 4. Finally, individually packaged commercial components make the volume of the combined Input/Output (I/O) units much larger than could be achieved if custom designed chips are used [Ref. 68].

Figure 4; Fiber Optic Cable Comparison. The photo shows standard 3.5" ducts carrying, respectively, 320 twisted wire pairs, 20 coaxial cables, and 5 optical fibers. Each has approximately the same information carrying capacity. [Ref. 69]

63

The major issue in fiber optic technology concerns the optical modulators which externally vary the optical carrier from the laser. Variables include cost, bandwidth and insertion losses. $LiNbO_3$ is the most dominant material for these devices because of its relatively low (3-7 dB) insertion loss. Semiconductors are also used; they have wider bandwidths (~60 GHz), but insertion losses are higher, ~10 dB. Because of their low cost and convenient packaging, polymers provide are another modulator material choice. [Ref. 11].

Exploratory research into other advantages offered by optics is driven by the need to achieve among other things, accurate beamsteering [Ref. 2]. Most electronically scanned arrays utilize phase shifters to direct the antenna beams. The RF energy is in phase, but does not arrive at the wavefront of the pointing direction at the same time. As a result of slight time delays, the arrays become skewed at high angles off broadside. The resulting beam direction is quite frequency dependant, precluding aiming of wideband signals in a single accurate direction. [Ref. 70]

In true time delay (TTD) steering, the RF energy from each radiator arrives at the wavefront of the antenna pointing direction at the same time and phase. TTD beamsteering utilizes optoelectronic components to achieve the wide instantaneous bandwidth needed in active arrays and is therefore, frequency independent. The antenna array pointing is correct far all frequencies for a given time delay setting.

64

Thus, TTD can be used with no change in setting or degradation in direction for a given pointing beam and provides accuracies to within milliradians. The beam steerer can be located at any convenient place in the manifold, either within the antenna array, adjacent to or within the T/R module, or wherever the RF signals are generated. [Ref. 2]

There are several ways that an optoelectronic TTD beamsteerer can be configured; laser, photodiode detector, or optical switches. Any of these allow the selection of different fiber cable lengths to achieve the desired delay. Both the laser and photodiode act as switches by respectively controlling their bias current or voltage while performing their typical functions of light generation and modulation, or detection when they are biased on. Pure optical switches(light input and light output) use electronically activated switches. Hybrid switches combine the best features of each of the three. [Ref. 2]

B. PHOTOGRAPHIC CAMERAS

Resolution, an expression of the optical quality of an image, is the biggest concern in maritime surveillance photography. It is influenced by many variables, including film and camera resolving power, uncompensated motion, and atmospheric conditions. The resolution of a given film is primarily dependent on the size distribution of the silver halide grains in the emulsion. Generally, the higher the granularity, the lower its resolving power. However, there

65

must be a compromise between resolution and speed (the film's sensitivity to light), which requires high granularity. [Ref. 71]

One new technique of resolution enhancement uses mean field annealing. It begins with a series of low resolution frames of the same scene, with each frame offset by a subpixel displacement. An advantage over other techniques is that knowledge of the exact displacement is not necessary. The high resolution reconstruction task is then formulated as an optimization problem, producing an increase in resolution of up to four-fold. [Ref. 72]

For comparison, two fairly well known satellites are presented; the Japanese Earth Resources Satellite (JERS-1) and the Satellite p'our l'Observation de la Terre (SPOT). Both are representative of current **unclassified** environmental observation platforms with optical sensor resolutions of 30.3m and 5m, respectively [Ref. 73, 74]. These systems are not nearly capable of providing the image quality required in maritime surveillance, as indicated in Table 3.

In the 1980s, RECONSAT, or KH-11, produced 6" (0.152m) resolution from an altitude of 248 miles. A new generation of Satellite Early Warning Systems (SEWS), including the KH-12, is expected to be deployed with still higher resolution. Interestingly, the theoretical resolution limit of satellite imagery is 3.9" (0.09m). [Ref. 75]

Object	Detection	Recognition	Precise ID	Description	Tech. Intel
Missile Sites	3	1.5	0.6	0.3	0.08
Radar	3	0.9	0.3	0.15	0.04
Aircraft	4.5	1.5	0.9	0.15	0.03
Nuke Weaps. Components	2.4	1.5	0.3	0.03	0.01
Surfaced Submarines	30.05	6.0	1.5	0.9	0.03
Vehicles/ Small Boats	1.5	0.6	0.3	0.05	0.03

Table 3; Resolution Required for Intelligence Interpretation
Tasks (meters) [Ref. 76]

C. INFRARED SENSORS

The importance of infrared (IR) surveillance has recently increased in part because of the emphasis on covert and low intensity operations. IR passively penetrates smoke, haze and some atmospheric moisture.

Infrared radiometry is based on the use of photodetectors to collect energy in two primary bands or "windows"; the 3-5 micron and the 8-14 micron bands. The 3-5 band suffers somewhat due primarily to attenuation by moisture. The 8-14 band is less sensitive and is better for detecting relatively cooler objects, but detectors in this band require cooling. Many of the newer systems employ dual bands. [Ref. 77]

67

Much R&D effort is directed at improvements in detector sensitivity, primarily through better materials. Lenses are usually constructed from germanium or silicon [Ref. 78]. Detector materials include platinum silicide, indium antomide and some silicons. Mercury Cadmium Telluride (HgCdTe) is popular because of its responsiveness at 6-12 micron range. [Ref. 77]

Solid state detector cameras can be classified into scanner or staring type. Focal Plane Array (FPA) cameras have a wider thermal range, higher operating temperature (cooling is less critical), greater reliability due to fewer moving parts, lower cost, better resolution, improved SNR and reduced signal processing requirements. FPA cameras however, do not give an absolute temperature reading and telescoping may not be available. [Ref. 78]

Current production photodetectors must be kept cool to remain sensitive to minor temperature variations. Though future technology will include uncooled thermal imagery, existing ambient temperature detector elements have not yet reached the same performance levels as cooled systems [Ref. 77].

The latest method of cooling eliminates the use of any gas or circulation pump and is termed thermo-electric (TE). Whereas Stirling or LN_2 have detector MTBFs of 2,000-4,000 hours, TE cooling improves it to 50,000 hours. Unfortunately, TE performance varies with ambient temperature and requires a fan which consumes more power than the pump associated with

Stirling cooling. Still, TE coolers are much cheaper and gaining popularity. [Ref. 78]

As is the case with radar, when the sensors reach their limits, efforts are directed at improvements in signal processing. Whereas currently fielded systems only use spatial filtering, computational capabilities now enable use of complex algorithms such as 3-D matched filters for detection and multiple hypothesis tracking (MHT) for tracking and data association.

The 3-D velocity matched filter bank discriminates between target and background returns based on their different spatial and temporal correlation properties. This matched filtering process whitens the clutter and noise that remains after processing and increases the SNR. [Ref. 79]

The MHT algorithm is effective at establishing tracks on dim targets in a heavy clutter or false alarm background. Each track has a score, a measure of the likelihood that the set of observations in the track are from the same source. The score is initially set to zero at the time of the first observation. Thereafter, each track's score is updated upon each scan and histories are recorded. Individual tracks are tested for confirmation and deletion using threshold tests which are based on system parameters and the false track confirmation requirements. A clustering method identifies and merges interacting/similar tracks. Those that survive the individual deletion tests are formed into hypotheses. [Ref. 79]

69

Once the system decides that a hypothesis is a target, two main design issues relate to false targets. First is the false track confirmation rate requirement. Tentative tracks must be formed on most of the many false alarms. Second is computer resources which limit the number of false tracks that can be maintained. Additional design tradeoffs include allocation of resources between signal processing and tracking complexity, detection threshold choice, and time-on-target/revisit time. The typically high false alarm rate for IR systems makes the last tradeoff even more complex. [Ref. 79]

Results discussed here primarily address track detection and confirmation. For IR systems, this is considered a more difficult problem than track maintenance. The MHT method rarely loses a track once confirmation occurs, even if the SNR decreases. Experimental performance is based on a hypothetical IR tracking system; 100 degrees in azimuth coverage, 4 false tracks/hour limit, 0.1 mrad pixel size, 50 velocity filters in the matched velocity filter bank and assorted probabilities of detection and false alarm (P_d and P_{fa}). [Ref. 79]

Simplified Monte Carlo simulations concluded that a threshold setting such that P_d is about 0.75 optimizes track confirmation performance. Also, there is a tendency toward requiring a lower false alarm rate as the required coverage increases and as more frames are used in the matched filter (so that false alarms can be reduced). Therefore, the

70

requirement to search a broader area may actually lead to a slower sensor scan rate. Another test determines the effects of target maneuver mismatch upon track confirmation performance. Results clearly indicated it is better to be conservative and ensure an adequately large maneuver window in the system's filter model. In a final test, it is found that the cost of operating with a true false track confirmation probability which is below the requirement results in a potential increase in the target track confirmation time. More succinctly, the time required for track confirmation increases dramatically as the sampling interval increases. [Ref. 79]

III. PLAYERS AND PRODUCTS

Tables 4 and 5 contain summaries of some of the major radar, IR and photographic manufacturers in the world. The tables are far from exhaustive; those companies included typically have several products applicable to maritime surveillance, are a major manufacturer in their respective country, or are developing new/interesting products. Addresses, phone numbers and a brief description of each manufacturer's market position are included.

Table 4: Major Radar Manufacturers

Company	Address Phone/Fax	Products	Performance	Application	Market Focus
Elta Electronics Industries Ltd.	Box 330 Ashdod 77102 Israel 972-8055-30333 F:972-8-563933 -563930	AT-101A	E/F, I/J, D-Band, stabilized cosec antenna w/switchable polarization	Ship & mobile land surveillance	The major manufacturer in Israel. Wide variety of products.
		EL/M-2228-S	S-Band, 16.3 nm, velocity coverage: .3-3 mach, multi-beam array	3-D Shipborne air surveillance. & missile detection	
		EL/M-2075 (Phalcon)	D-Band, 250 nm, multi-mode, conformal phased array w/liquid cooled T/R modules	AEW (Boeing 707)	

Company	Address Phone/Fax	Products	Performance	Application	Market Focus
GEC Marconi Def. Syst. Ltd. Nav. & Electro- opticDiv.	Ferry Rd. Edinburgh EH5 2SX 44-31-343-4509 F:44-31-343-4507	Blue Kestrel	I-Band, coherent, multi- mode, selectable PRF/PW, planar array antenna	Helo maritime surveillance	One of two major manufacturers in the U.K. Wide variety of products.
		Sea Spray	"	"	
Radar Systems Ltd., Marconi Research Center	Writtle Road Chelmsford Essex CM1 3BN U.K. 44-245-267-111 F:44-245-357-927	Type-1022	D-Band, squintless-feed antenna	Long range air & surface surveillance	
		S810	8.6-9.5 GHz, PRF: 1500/ 4400 Hz, PW: .67/.33 us. stabilized elliptical ant.	Shipborne air/surface search	
		S820	2.7-2.9/2.9-3.1 GHz, PRF: 750/1500 Hz, PW: 1.2/.6 us. stabilized elliptical antenna	Shipborne air/surface search	
		S1820	E/F-Band, 57 nm, 2 kW peak, 800 W mean, stabilized elliptical antenna	Shipborne air/surf. tactical surveillance	

Company	Address Phone/Fax	Products	Performance	Application	Market Focus
Hughes A/C	El Segundo, Ca (310)334-4050 F:(310)334-6278 (James Lemon) (310)334-6687	ASARS-2 ---------- TR-1A ---------- HISAR (Hughes Integrated SAR) ----------	no perf. data available ----------------- no perf. data available ----------------- Real-time X-Band, multi-mode, 65 nm. -----------------	SLAR ----------- ----------- Airborne SAR surveillance -----------	Shifting focus to short range littoral warfare, space-based surveillance, and overseas sales.
	Box 3310 607/B219 Fullerton, Ca 92634 (714)732-5093 (Chic McDaniel)	TAS MK-23	Pulse-doppler L-Band, multi-mode, 20/90 nm., horn-type vert. polarized antenna	2-D Shipborne surveillance. & missile detection	
Litton Syst, Canada, Ltd.	25 Cityview Dr. Etobicoke, Ont. M9W 5A7 (416)249-1231 Malcom Stanton	APS-504(V)5	8.9-9.4 GHz, 8 kW peak, multi-mode, 200 nm	$1.2 million airborne maritime surveillance (inexpensive APS-140 follow-on).	Major supplier to Canadian Navy and Coast Guard
Lockheed Martin	Electronics Syst. Div. French Road Utica, Ny 13503 (315)739-7708 F:(315)793-7711	APS-145	350 nm range	AEW (USN E-2C)	Major radar supplier to USN AEW aircraft.

Company	Address Phone/Fax	Products	Performance	Application	Market Focus
McDonald Dettwiller Technologies	13800 Commerce Pkwy, Richmond, BC V6V 2J3, Canada (604)278-3411 F:(604)278-2117	IRIS (Integrated Radar Imaging System)	multi-mode	SLAR reconnaissance	
Mitsubishi Electric Corporation	Mitsubishi Denki Bldg. 2-Chrome 2-3 Manouchi, Chiyoda-Ku Tokyo 100 81-3-3218-3340 F:81-3-3218-2924	OPS-24	D-Band, 90 w peak, T/R modules (trans:40 dB gain, rec:28 dB gain), hybrid active array	Shipborne air surveillance.	

77

Company	Address Phone/Fax	Products	Performance	Application	Market Focus
Motorola Government & Systems Tech. Group	8220 E. Roosevelt St. Box 9040 Scottsdale Arizona 85252-9040 (602)244-6900	APS-131	X-Band, 200 kW peak, PRF: 677/1477, PW:.2 us, vertically polarized slotted waveguide array	~$1.0-1.5 million SLAR surveillance. (USCG HU-25A)	Major radar supplier for USCG aircraft.
		APS-135	" "	SLAR surveillance. (USCG HC-130, Boeing 737)	
		SLAMMR	X-Band, 27 nm MTI, 189 kW peak, 60 W avg, 37 dB gain slotted waveguide antenna	SLAR surveillance. (Border Patrol C-130)	
		APS-94 mod	Range: 64 nm	SLAR surveillance. (USCG C-130)	
NEC Corp.	7-1 Shiba 5-Chrome Minatu-Ku Tokyo 108-01 (813)3789-6531 F:(813)3798-1510	NPG-880	no perf. data available	Land based 3-D air def.	Land-based radars
		J/TPS-102	no perf. data available	Mobile land-based air def.	

78

Company	Address Phone/Fax	Products	Performance	Application	Market Focus
Raytheon Co. Equipment Div.	528 Boston Post Rd. Sudbury, Ma. 01776 (508)490-1000 F:(508)490-2822 Michael Sosin (508)440-4945	SPS-49(V)5	850-942 MHz, 36 kW peak, 13 kW avg, mult. PRF, 28.5 dB gain cosec² antenna, total weight: 17,169 lbs.	2-D Long range shipborne air search	
Siemans-Plessey, Microwave tech group	Cowes, Isle of Wright, U.K.	AWS-6e -------- AWS-9 -------- MESAR	air surveillance: 38 nm, missile det: 19 nm. -------------------- Multi-mode, E/F-Band -------------------- no perf. data available	3-D Shipborne air/surf. surveillance. ----------------- " " ----------------- Active phased array	One of two major manufacturers in the U.K.
Telstra applied tech.	Module 1 Endeavor House Technology Park South Aust. 5095 ------- 35 Winterton Rd. Clayton, Victoria 3168, Aust. 613-541-6000 F:613-562-7745	Jindalee	HF Band, 540-2170 nm., position resolution: 11-22 nm, bistatic antenna	OTH	Jindalee is the definitive land-based OTH radar.

79

Company	Address Phone/Fax	Products	Performance	Application	Market Focus
Texas Inst. Inc.	Box 255012 M S 57 Dallas, Tx. 75265-5012 (214)995-2011 F:(214)995-4360	APS-134+ ---------- APS-137	multi-mode ------------------------------- 9.75 GHz nominal center freq., inst. BW: 500 MHz 50 kW peak, 500 W avg., PRF: 5000 Hz, PW:10 us.	Airborne ISAR maritime surveillance ------------------------ " "	Major supplier for USN maritime surveillance aircraft (P-3s & S-3s).

Company	Address Phone/Fax	Products	Performance	Application	Market Focus
Thompson CSF Div. Systemes Def et Control	18 Ave de Marechal Juin, BP 34, F-92360 Meudon- la-Foret, France 33-141-07-5000 F:33-141-07-5019	DRBJ-11:	E/F-Band, active phased array	Shipborne air search/ target designator	The major French manufacturer & research center. Wide variety of products. A sea- clutter research leader.
		TRS-3050 (Triton -G)	G-Band, 10 nm, 27 dB gain antenna	Shipboard air/surface search	
		Sea Tiger (DRBV-15C)	E/F-Band, 60 nm, 30 dB gain, switchable polarization antenna	Air/surface surveillance	
		DRBV-26C (Jupiter-S):	D-Band, 144 nm, cosec^2 antenna	Shipborne air surveillance	
		TRS-3405:	I-Band, 200 kW peak, PRF: 570-1080 Hz, inverted cosecant antenna	Land-based coastal surface search	
	7rue des Mathurins 92223 Bagneux, France	TRS-3010 (Jupiter)	D-Band, 2 MW peak	Shipborne long range multifunction	
		Oceanmaster 400	I/J-Band, PRF: 300-30 Hz, 200 nm, 8 kW max, .4 kW avg, offset reflector antenna	Airborne maritime surveillance	
Div. Radars et Contre-	178 bd Gabriel Peri	Iguane/ Agrion	I/J-Band, SLAR	Airborne maritime surveillance	

Company	Address Phone/Fax	Products	Performance	Application	Market Focus
Westinghouse Electronic Syst. Group Aerospace Div.	Box 746 Baltimore, Md. 21203 (410)765-1000 J. Standish (410)765-2900	APY-1/APY-2	10-cm Band, multi-mode	AEW (USAF AWACS E-3/ Boeing 707 &767). Multi-billion $ package for NATO, sale to Japan likely	
		AN/SPS-65(V)ER	1215-1400/5255-5925 MHz, 25 kW peak, 61 nm range, planar dipole array	Shipborne search, production is winding down	
		E-LASS (Enhanced Low Alt. Surveillance System)	1.25-1.35 GHz, 160 nm, PRF: 774 avg, PW: 39 us, 100 kW peak	Aerostat-borne (balloon), anti smuggling surveillance (U.S. Customs). $35-40 million for sensor & platform package	

82

Company	Address Phone/Fax	Products	Performance	Application	Market Focus
Westinghouse/ Norden	Norden Place Box 5300 Norwalk, Conn. 06856 (203)852-5000 F:(203)852-7480	APQ-173:	no perf. data available	Airborne search/attack (A-6E, cancelled)	Sensor fusion systems (ie: Joint STARS)
		-------------	-------------------------------	-------------------------------	
		AN/SPS-40E	400-450 MHz, 130 kW peak, 2 kW avg, PW: 60 us (long range)/3 us. (short range), open lattice antenna	Shipborne search	
		-------------	-------------------------------	-------------------------------	
		AN/SPS-67(V)	G/H-Band, multi-mode	Shipborne search	
		-------------	-------------------------------	-------------------------------	
		Joint STARS	no perf. data available	Airborne surveillance. & battle management system (E-8A/ Boeing 707)	

Table 5: Major IR/Photographic Manufacturers

Company	Address Phone/Fax	Products	Performance	Application	Market Focus
Boeing Defense & Space Group	Box 3999 Seattle, WA 96124-2499 (206)773-2816 F:(206)773-2113 Heather Shaw	Airborne Surveillance System (AST)	38,400 IR detectors, cryogenically cooled	Airborne long range IR sensor	
FLIR Systems, Inc.	16505 S.W. 72nd Ave. Portland, OR 97224 (503)684-3731 F:(503)684-5452	AN/ALQ-22 (SAFIRE) ------------- Situational Awareness FLIR	fov: 28°x16.8°,5°x3°, 40 kg. -------------------- 30 frames/sec., 8-12 microns, 28°x15°, 10 kg.	Airborne IR system --------------------- " "	
GEC Marconi	Christopher Martin Rd. Basildon, Essex SS14 3EL, U.K. 44-126-852-2822	Sea Owl IR sensor	8-13 microns, mag: 5x-30x, 103 kg.	Maritime surveillance helicopter-mounted (Royal Navy's "Lynx")	
Lockheed Aeronautical Systems Co.	86 South Cobb Drive, Marietta, GA. 30063 (404)494-4411 F:(404)494-6263 Dave Bork	SAMSON IR/TV/photo pod	no perf. data available	Airborne drug interdiction, SAR, treaty verification	Recent merger w/ Martin Marietta.

84

Company	Address Phone/Fax	Products	Performance	Application	Market Focus
Lockheed Fort Worth Co.	Box 748 Fort Worth, TX 76101 (817)777-2000 F:(817)777-2115 Joe Stout (817)763-4084	Low Intensity Conflict Aircraft System (LICAS)	360° FLIR, IR line scanner, multispectral camera, off-the-shelf hardware, 347 kg.	Cessna cargo pod-mounted, Drug interdiction, border/coastal surveillance	"
Loral Fairchild Systems	300 Robbins Lane, Syosset, NY 11791 (516)349-2200 F:(516)931-4037	AN/ADV-5 (LOROPS)	FPA: 12,000 pixels, range: 30 naut. mi., 1000 lbs.	Long range oblique camera for airborne reconnaissance	One of two U.S. surv. camera manufacturers.
		SU-172	medium alt. sensor, multiple focal lengths, 62 kg.	Airborne reconnaissance camera	
		SU-173	low alt. (200'-10,000') electro-optic camera, 25 kg.	Airborne reconnaissance camera, UAV-mounted	
Loral Infrared and Imaging Systems	2 Forbes Rd. Lexington, MA 02173 (617)862-6222 F:(617)863-3496 Bill Collins (617)863-3035	Stabilized Thermal Imaging System	mag: 12x, 2 bar sprite detector, fov: 20°x30°, 7.2°x10.8°, 2°x3°, 8-12 microns, 34 kg.	Fixed wing a/c, helos, and UAV-mounted	
		LTC500	327x245 FPA, 3 kg.	Uncooled short range IR surveillance camera	

Company	Address Phone/Fax	Products	Performance	Application	Market Focus
Martin Marietta Electronics and Missiles Co.	Orlando, FL 32819-8907 (407)356-2211 F:(407)356-2080 Andrea Lawrence	Electro-Optic Sensor System (EOSS)	FPA IR sensor coupled to pilot's line-of-sight (sensor fusion), TV: 0.65-1 micron, IR: 8-12 microns, 204 kg.	RAH-66 Comanche helicopter	Recent merger w/ Lockheed.
Recon/Optical Inc.	550 W., N.W. Highway, Barrington, IL 60010-3094 (312)381-2400 F:(312)397-2214	KS-146/147 ------------- KS-157	66" f5.6 lens, 10-50 naut. mi. range @ 30,000' ------------------------- 66" f5.6 lens, 5-75 naut. mi. range @ 50,000', 3' res. @ 60 naut. mi.	Airborne Reconnaissance Camera ---------------------- "	One of two U.S. surveillance camera manufacturers.
Rockwell Intx.	3370 Miraloma Ave., Box 3105 Anaheim, CA 92803 (714)762-1569 C.L. Hayes	LADAR/ Radiant Outlaw	HdCdTe FPA, 256x256 pixels, Neural network based target recognition	Airborne IR, visual imagery and LASER ranging package	

Company	Address Phone/Fax	Products	Performance	Application	Market Focus
Texas Inst. Defense Systems & Electronics Group	Box 660246 8505 Forest Lane Dallas, TX 75266 (214)480-1417 F:(214)480-3281 Vicki Fendlason	AN-AAQ-17 ------------- RPV-800 ------------- T-Sight	IR detector, fov: 13.7°x18.3°, 3°x4°, 68 kg. ---------------------------- real-time data-link video, spatial res: 0.5 mrad, 13.6 kg. ---------------------------- uncooled, 8-12 microns, range: 1000 m	Airborne SAR, navigation, fire control ---------------------------- UAV mounted IR line scanner ---------------------------- $25,000 hand-held IR detector. Sold to Australian military & possibly USMC	Major supplier for USN maritime surveillance a/c.
Thompson-TRT Defense Optronics Division	rue Guynemer, Box 55, F-78283, Guyancourt Cedex, France 33-1-92-96-3000 F:33-1-92-96-4630	AA3-38-100 ------------- Tango thermal imager	range: 9-100 km, res: 1 m @ 100 km, lens: 1700 mm autofocus, frame rate: 1.67 frames/sec, 350 kg. ---------------------------- passive ship/snorkel detection, fov: +/- 110, 85 kg.	Reconnaissance camera ---------------------------- Developed for the Atlantique-2 (French maritime patrol a/c)	The major IR/photo manufacturer in France.
Thorn-EMI	120 Blyth Rd. Hayes, Middlesex UB3 1DL, U.K. 44-181-573-3888	Multirole Thermal Imager	HdCdTe FPA, 8-13 microns, fov: 4.9°x3.2°, 12.9°x8°, 23 kg.	Airborne off-shore patrol and surveillance	

87

Company	Address Phone/Fax	Products	Performance	Application	Market Focus
Westinghouse Electric Corp.	Box 17319 MSA255, Baltimore, MD 21203 (410)993-6454 Tom Delaney	WF-360 IR/TV system	360°, mag: 11x, sensitivity: .1°c, 355 hours MTBF, TV res.: 500 TVL/P, TV sensitivity: .02 LUX	SAR, drug interdiction (USCG HU-25, USAF C-26, US Army)	Major IR system supplier to USCG.
		NIGHTGIANT (IR, LLTV, daylight TV)	40x mag, closed cycle cooling, 480x4 FPA, 625 line video, LLTV sensitivity: 10^{-5} LUX	Long range surv. system used by USAF and UAVs.	
W. Vinton, Ltd.	Vicon House Western Way Bury St., Edmunds Suffolk, IP33 3SP U.K. 44-128-475-0599	Type-401 Line Scanner	8-14 microns, res: 1 mrad., fov: 120°	Airborne reconnaissance, exported to ~20 countries	Wide variety of photo products.

In addition to their current products, manufacturers are continually developing new designs and refining old ones. For example, microwave monolithic integrated circuit technology has advanced to the mass production stage. Currently, all major radar developers have active array radar programs in progress. [Ref. 8]

In 1994, **ITT** delivered airborne T/R modules for the US Navy. The cost per module has decreased significantly during the production run due to increasing yields. The module's output power is 13.8 W @ 34.6% PAE. **ITT** currently manufactures MMIC chips under contract to ARPA/US Army that contain all microwave functions on a single chip producing up to 4 W output power. The T/R module output power can be increased to over 10 W by a high power amplifier (HPA) at the output of the T/R chip [Ref. 8]. Meanwhile, **Thompson-CSF** is scheduled to produce several thousand T/R modules by 1996 for a joint active radar project with **G.E.**, **Siemens** and **Thorn-E.M.I**. [Ref. 80]. Additionally, researchers at **Hughes Aircraft** are proposing the construction of a 2,000 module fiber optic array weighing under 75 pounds and less than 2" thick. For comparison, a comparable non-fiber optic design is about 12" thick and weighs several hundred pounds [Ref. 2]. Finally, the **European Space Agency** (ESA) plans to launch POEM-1 (Polar Orbiting Earth Mission) in 1998. The satellite contains a SAR-type space-based radar with 320 T/R modules, each with stringent size, mass, power consumption and performance specifications [Ref. 9].

89

Sensor fusion is the integration of radar with optical, IR and even visual capabilities. **Rockwell-Collins** and **Thompson-CSF** are currently assessing the benefits of millimeter-wave radar to assist pilots in landing and taxiing aircraft under low visibility conditions. In the proposed system, radar images are presented to the pilot on a Heads-Up Display (HUD). One issue that must be addressed is the question of bore-sighting the system so that radar images on the HUD are accurately aligned with the real world. [Ref. 81]

While NATO AWACS aircraft provide airborne surveillance and command & control for all allied NATO forces, U.S. AWACS are dedicated to counter drug and contingency operations. The E-3 Radar System Improvement Program (RSIP) is a plan to significantly improve AWACS radar detection range, Electronic Counter Counter Measures (ECCM) capability, reliability and maintainability. As the plan currently stands, **Boeing** and its major subcontractor, **Westinghouse** will produce modification kits for 18 NATO and two U.S. AWACS with options for 11 additional kits. Some of the components may be procured from firms in Europe or Canada. Total program cost is $487.9 million. [Ref. 82]

Unmanned air vehicles are being fielded by several manufacturers. **Lockheed** displayed their Tier-3 Minus reconnaissance drone on June 1, 1995 and will begin flight testing in late 1995. It is designed to carry either a **Westinghouse** SAR or **Recon/Optical Inc.** electro-optical sensor. Data and commands can be relayed via ground station

90

or Ku-Band commercial satellite. It has a 500 nautical mile range and an eight hour loiter time. [Ref. 83]

The USAF plans to purchase 20 Joint-STARS systems to support contingency and counternarcotics operations as well as joint training [Ref. 84]. Additionally, **Northrop-Grumman** is joining with **Motorola** and nine European companies to build 18 Joint-STARS Boeing 707s for NATO use. Total cost for the NATO acquisition is estimated to be $4.7 billion [Ref. 85]. One of Joint-STARS' original contractors, **Westinghouse Norden Systems,** proposes a new interferomic SAR processing technique which is capable of creating moving target images of ground objects while suppressing clutter. In tests, interferomic moving target focusing (IMTF) gives one-meter range resolution and may further aid target identification by detecting target vibrations. IMTF can easily be implemented into the Joint-STARS system. [Ref. 86]

Texas Instruments is developing a derivative of its APS-137 maritime surveillance radar for Canada's new shipborne helicopter, the EH-101. The radar is designed to accept a later ISAR upgrade capability. The $70 million contract stipulates thirty-five systems are to be delivered, starting in 1996. [Ref. 87]

A five country (Germany, France, Italy, Spain and U.K.) consortium is developing a new maritime patrol aircraft known as Europatrol. It will replace the Atlantique 2 [Ref. 88]. In another European maritime surveillance platform purchase, the French Navy has ordered 15 AS565 Panthers (a dual-engined

91

military version of the Dauphine civil helicopter) for various roles aboard its frigates. Delivery dates are between 1993 and 1997. **Aerospatiale** produces the Panther, which is already used by the U.S. Coast Guard for search-and-rescue missions. [Ref. 88]

Passive infrared tracking equipment (PIRATE) will be employed on the European fighter aircraft (EFA). It is an IR system which detects and automatically tracks multiple air and ground targets using three separate signal processors. PIRATE is required to provide identification at ranges exceeding radar as well as detect hostile missile launches through perception of heat plumes [Ref. 77]. PIRATE range is classified, but is conservatively expected to exceed 30 nautical miles [Ref. 77]. Another long range IR system is the **NASA**-sponsored, RU-2 mounted Airborne Visible-Infrared Imaging Spectrometer (AVIRIS), which was used to calibrate the optical sensor aboard the JERS-1 satellite's optical sensor. AVIRIS' high spectral resolution and validated calibration provided the basis for its use. [Ref. 89]

AVIRIS specs:[Ref. 89]

wavelength range:	0.4-2.5 microns, 0.01 micron increments
field of view:	30 degrees; 11 km @ 20 km above ground
flight line length:	up to 10 100 km flight lines
calibration:	<.001 microns

The merger of **Lockheed Corp.** and **Martin Marietta** has produced a research and development giant, according to the DoD's list of top 500 research, development, test and evaluation (RDT&E) contract winners in 1994. Several of those involved in maritime surveillance-related work are listed in Table 6:

Rank	Company	Dollars (in thousands)
1	Lockheed Corp.	2,643,730
2	Martin Marietta Corp.	1,820,572
4	Northrop-Grumman Corp.	935,138
6	Raytheon	534,180
10	Mitre Corp.	414,447
11	G.M. (Hughes)	395,191
13	Loral Corp.	376,417
16	Mass. Inst. of Tech.	313,151
20	Texas Instruments, Inc.	251,424
25	Westinghouse Electric Corp.	198,534
29	Boeing	123,394
39	Israel Aircraft Industries, Ltd.	86,933

Table 6; Major US DoD RTD&E Contract Awardees with Ties
        to Maritime Surveillance Technologies. [Ref. 90]

In addition to those organizations previously discussed or listed in the tables, many others are currently studying

maritime surveillance problems and proposing solutions. **Litton Systems, Canada** is producing much research on the topic of sea clutter. The **EE and CS departments at Syracuse University** are also studying clutter. The **Georgia Tech. Research Institute** is investigating airborne and ground clutter as well as sensor fusion. **Rome Labs (Griffiss Air Force Base)** is producing research in sensor fusion, STP and artificial intelligence for false alarm processing. **Elta Electronics Industries, Ltd.** is involved in SAR MTI and the **Naval Research Lab, Radar division** is studying ultrawideband radars and phased arrays for low altitude targets.

IV. OPPORTUNITIES

The following applications exemplify maritime surveillance needs and show how some of the previously discussed R&D efforts are likely to be incorporated.

A. LITTORAL WARFARE

Littoral warfare is characterized by many contacts in a relatively small area. A sensor's long range is not as important as the ability to quickly and positively identify contacts in clutter, whether they be hostile, friendly, or neutral. Electronic jamming is virtually guaranteed. Quick sensing and reactions are vital. Platform endurance is less of an issue.

Whether ship, fixed-wing or helicopter based, wideband and ultrawideband radars can solve some of the above stated problems. They are relatively jam-resistant, reject clutter well and lend themselves to the imaging problem. Millimeter-wave radars are also effective over the relatively short ranges. ISAR's imaging capability has already and will continue to provide positive identification, with enhanced speed and accuracy, thanks to faster signal processing algorithms and software refinements. Additionally, fusion of radar and IR sensors will help ATR systems with the identification problem. Upgradable databases will ensure current target signatures are available. Finally, AESA antennas allow radars to target specific contacts while simultaneously searching elsewhere.

B. LAW ENFORCEMENT/CUSTOMS

In these operations, the ability to positively identify small surface and/or airborne contacts is critical. Almost as important is the ability to remain covert, or at least appear nonthreatening. Endurance (specifically long range coupled with long loiter time) is also vital. Contacts are usually neutral, but may become evasive or even belligerent. Jamming is unlikely, but not out of the question.

Again, ISAR and wideband radar fulfills the positive identification requirement. AESA antennas will allow radars to identify the contacts while continuing uninterrupted surveillance. As these arrays become lighter weight, they can be mounted high on a ship's mast, increasing the range. IR's passive nature helps maintain the nonthreatening profile. Unmanned air vehicles (UAVs) and aerostats, because of their extended endurance in a relatively benign environment, are being successfully tested and fielded for long range surveillance in general and this mission in particular.

C. SEARCH AND RESCUE

This mission has slightly different requirements. It typically involves one or a small number of contacts. High seas, foul weather and the attendant clutter are often a major concern. However, positive identification and pinpoint accuracy are not as critical. Contacts are less likely to be hostile and jamming is not usually an issue. Platform endurance is, as before, important.

96

Wideband radars and their ability to cut through clutter are once again a viable approach. Additionally, advanced ADCs, SAW pulse compression and scan-to-scan processing technologies enable detection of small objects in clutter with a high degree of reliability. Fusion of radar, IR and optical systems is another applicable technique.

D. MARITIME/COASTAL PATROL

This encompasses all of the above missions. Thus, the platform's flexibility is as important as its sensors' capability. In addition, aircraft and satellite based SAR imaging supplemented with MTI can provide vital reconnaissance information.

E. AIR TRAFFIC CONTROL AND HARBOR CONTROL

These usually employ permanent ground based equipment and therefore, have fewer design constraints. Long range is not particularly important. Instead, precision, accuracy and reliability are by far the most pressing concerns.

Multimode active array ATC systems using MMIC technology are already being fielded and upgraded versions will no doubt follow. Multiple T/R modules' redundancy and graceful degradation characteristics help to ensure a high degree of reliability. Millimeter-wave radars tend to be short but accurate, making them excellent candidates for close range systems. TTD and digital beamforming technologies are other keys to enhance both steering precision and accuracy. Global

97

positioning system (GPS) is a supporting technology that is important to have in the other scenarios and absolutely critical in air traffic and harbor control.

F. LAND BASED COASTAL SURVEILLANCE

These systems require powerful, long range hardware. Additionally, a significant amount of signal processing is required to peer through the clutter, reflections and ionospheric effects. Simple detection is more important than resolution or precision.

There are several of these long range air defense type radars in development as well as those already operational. Bistatic antennas and ultrawideband technology are key factors in their employment. However, coastal surveillance radars' popularity has leveled since the cold war's end, primarily because they are expensive and inflexible. Additionally, new threats could render them useless overnight. Finally, their effectiveness against stealthy aircraft and missiles is questioned.

G. AIRBORNE SURVEILLANCE/EARLY WARNING

This mission requires a platform with a very long loiter time such as the USAF AWACS and USN E-2C. Systems must be powerful to achieve long ranges as well as capable of multiple target tracking. Precision and accuracy are key. Electronic jamming is to be expected.

AESA antennas, with their MMIC technology, multimode capability and fiber optic connectors, are perfect for this mission. ECCM enhancements must be incorporated to resist jamming. Additionally, enhanced signal processing capability supplemented by an extensive communications suite allows for rapid dissemination of refined target information.

100

V. CONCLUSIONS AND SUMMARY

It is no longer enough for maritime surveillance systems to determine range and bearing to a contact. Modern sensors must have the capability to detect, identify, determine altitudes, track multiple contacts at hypersonic speeds, and establish threat priorities. Data integration and quick response are also critical. Automatic target recognition systems are becoming essential to survival.

The era of the phased array radar is in full swing. Much development effort has been given to AESA antennas, which have large numbers of T/R modules directly behind the array face, often connected by fiber optic cables. Most current active arrays are heavier than passive antennas, posing limitations with naval radars where mounting is normally high on the ship's mast. However, the advantages far outweigh the disadvantages and active arrays are expected to appear in both air and shipborne applications in the late 1990s [Ref. 78]. Supplemented by digital beamforming techniques for array steering and control, active arrays will revolutionize radar systems. The favored method of constructing electronically steered arrays is with MMIC devices using GaAs based substrates. MMIC chips are now coming into operational use. Research continues in the areas of design and manufacturing technology, emphasizing high volume and low cost production.

Smart skins, active antennas built into the airframe, are being investigated to combat the problems of space, radar cross-section and aerodynamics. However, the technique is

101

very difficult since the T/R modules must be part of the load bearing structure. Unfortunately, they cannot be made from carbon-fiber composites because the graphite in the composites attenuates RF radiation. Thus, with the possible exception of a small number of "high end" aircraft, this technology is not expected to be fielded soon. Other developments that can be confidently predicted include the use of polarization and wideband technology to better identify radar targets, especially in clutter.

The sea-skimming missile or low flying hostile aircraft presents a problem to ship based surveillance systems, which are largely range limited due to antenna height and weight. Smaller, higher frequency radars may be a solution. For short range applications, millimeter wave and IR systems are likely to become more widespread. Though limited to line-of-sight range, IR is much less vulnerable in hostile environments. There is also a move toward the use of sensor fusion, wherein radar is automatically blended with IR and optical systems to establish the best classification possible. While a single sensor may not provide reliable identification, synergistic data fusion gives a complete surface and air picture. Concern over IFF is a problem that has not yet gone away. But, with the development of sensor fusion, it too, may be solved.

Satellite-based radar has been used for several years; most systems are based on SAR techniques. They appear to be quite good at detecting ballistic missiles, but are expensive to manufacture, launch and maintain, and so far, have found

more use in commercial applications than military [Ref. 66]. On the other hand, integrated SAR based systems used in airborne surveillance and targeting are being successfully developed and fielded. The Joint-STARS system was very effective in the Gulf War and may be the most well known. Balloon-borne radar has reappeared for drug enforcement and high endurance, long range coastal surveillance. The next technological hurdle for air defense radar systems to overcome is the development of a means of stealth aircraft detection. Bistatic over-the-horizon (OTH) radars appear to be the most likely solution. The use of UAVs is a supporting technology with obvious advantages. Personnel are not put at risk and the vehicle can conduct extended, relatively covert surveillance with multiple real-time sensors. Long-term programs are in operation in both the U.S. and Europe.

Overall, militaries are spending more frugally, choosing to upgrade existing systems, especially software, instead of developing new ones. Nearly all countries made substantial reductions in their defense budgets, the exception being France, which has decided to remain one of the leading military powers and has made a slight increase in defense spending in 1994 [Ref. 67]. The United States still spends about $80 billion annually on weapons research and procurement, nearly twice the amount Japan spends on all of its defense. France and Britain spend even less, about $35 billion each [Ref. 91].

At the manufacturer level, these cutbacks in military spending have led to a number of mergers and takeovers in both the U.S. and Western Europe. Additionally, military procurement is becoming more reliant on research and products made outside the traditional defense industry. Microprocessors and anti-collision radars from the auto industry are two examples.

In summary, radar, supplemented by IR, will continue to be the major maritime surveillance sensor. It is a flexible and mature technology, capable of covering large areas in real time. Radar information will come from a wide variety of platforms, especially aircraft (both manned and unmanned). Fast data fusion, interpretation and dissemination will be a major challenge and will provide the most opportunities for improvement.

REFERENCES

1. Raffaelli, L., et al. "A Low Cost 77 GHz Monolithic Transmitter for Automotive Collision Avoidance Systems," *IEEE Microwave and Millimeter-Wave Monolithic Circuits Symposium Digest*, pp. 63-66, New York, 1993.

2. Newberg, I.L., and J.J. Wooldridge, "Revolutionary Active Array Radar Using Solid State 'Modules' and Fiber Optics," *Record of the IEEE National Radar Conference*, pp. 88-92, New York, 1993.

3. Lane, A.A., and F.A. Myers, "Advanced GaAs MMIC's for Phased Array T/R Modules," *IEE Colloquium on 'Phased Arrays' Digest*, pp. 7/1-7/4, London, 1991.

4. Hull, W.P. Jr., and R.D. Nordmeyer, "Active-element, Phased-array Radar: Affordable Performance for the 1990s," *National Telesystems Conference Proceedings*, vol. 1, pp. 193-197, 1991.

5. Chang, K.W., et al. "A W-band Single-chip Transceiver for FMCW Radar," *IEEE Microwave and Millimeter-Wave Monolithic Circuits Symposium Digest*, pp.41-44, New York, 1993.

6. Wang, H., et al. "A Monolithic Ka-Band 0.25 um GaAs MESFET Transmitter for High Volume Production'" *IEEE Journal of Solid-State Circuits*, vol. 27, no. 10, pp.1397-1404, 1992.

7. Maoz, B., et al. "FM-CW Radar on a Single GaAs/AlGaAs HBT MMIC Chip," *IEEE Microwave and Millimeter-Wave Monolithic Circuits Symposium Digest*, pp. 3-6, New York, 1991.

8. Brukiewa, T.F., "Active Array Radar Systems Applied to Air Traffic Control," *IEEE National Telesystems Conference Proceedings*, pp. 27-32, New York, 1994.

105

9.   Hector, C., et al.   "T/R Module MMIC Components for Spaceborne S.A.R.," *IEE Colloquium on 'Active and Passive Components for Phased Array Systems' Digest*, pp. 12/1-7, London, 1992.

10.   Richardson,   R.,   "Lightweight   Millimetric   Radar Transmitter," *IEE Colloquium on 'Millimetre-Wave Radar', Digest No.089*, pp. 6/1-4, Chelmsford, UK, 1990.

11.   Pace, P.E.   Personal Notes, 31 August, 1995

12.   Budzinsky, Y.A., and S.P. Kantyuk, "A New Class of Self-Protecting Low-Noise Microwave Amplifiers," *IEEE International Microwave Symposium Digest*, pp. 1123-1125, New York, 1993.

13.   Ewell, G.W., et al.   "Protection of Medium-Power Pulse Klystrons," *IEEE Conference Record of the 1990 Nineteenth Power Modulator Symposium*, pp. 44-51, New York, 1990.

14.   Mead,   J.,   and   R.   McIntosh,   "Pulsed   Polarimetric Millimeter-Wave Radars that Utilize Extended Interaction Amplifier and   Oscillator   Tubes,"   *1991   National Telesystems Conference Proceedings, Vol.1,* pp.343-346, IEEE, Amherst, 1991.

15.   Cormier, R.A., and A. Mizuhara, "250-kW CW Klystron Amplifier for Planetary Radar," *IEEE Trans. on Microwave Theory and Techniques*, vol. 40, no. 6, pp. 1056-1061, Pasadena, 1992.

16.   Bhanji, A.M., et al. "Conceptual Design of a 1-MW CW X-Band Transmitter for Planetary Radar," *Proceedings of the IEEE   International   Radar   Conference*,   pp.147-152, Pasadena, 1990.

17.   Freiley, A., et al.   "The 500-kW CW X-Band Goldstone Solar System Radar," *IEEE MTT-S Digest*, pp. 125-128, Pasadena, 1992.

18. Eaves, J.L., and E.K. Reedy, eds. *Principles of Modern Radar*, New York, Van Nostrand Reinhold, 1987.

19. Kitazume, S., and H. Kondo, "Advances in Millimeter-Wave Subsystems in Japan," *IEEE Transactions on Microwave Theory and Techniques*, vol. 39, no. 5, pp. 775-781, May 1991.

20. Ling, C.C., and G.M. Rebeiz, "A 94 GHz Planar Monopulse Tracking Receiver," *IEEE Transactions on Microwave Theory and Techniques*, vol. 42, no. 10, pp. 1863-1871, Pasadena, 1994.

21. Baldini, L., et al. "Performance Evaluation of a Multipolarisation Receiver," *IEEE International Conference on Radar 1992*, pp. 242-245, London, 1992.

22. Moyer, L.R. et al. "Analog Clutter Cancellation Algorithms for Dynamic Range Reduction," *IEEE AES Systems Magazine*, pp. 10-14, 1993.

23. Abidi, A.A. "Trends in High Performance Data Conversion," *International Symposium on VLSI Technology, Systems, and Applications. Proceedings of Technical Papers*, pp. 329-330, IEEE, Los Angeles, 1993.

24. Suresh Babu, B.N., and C.M. Sorrentino, "Analogue-to-Digital Converter Effects on Airborne Radar Performance," *IEE Proceedings-F*, vol. 139, no. 1, pp.73-78, Bedford, 1992.

25. Pace, P.E., et al. "Optical Sigma-Delta Analog-to-Digital Converters for High Resolution Digitization of Antenna Signals," *Proceedings of the 5th Annual Symposium on Photonic Systems for Antenna Applications*, pp. 412-416, 1994.

26. Pace, P.E., and D. Styer, "High-Resolution Encoding Process for an Integrated Optical Analog-to-Digital Converter," *Optical Engineering*, vol. 33, no. 8, pp. 2638-2645, Monterey, 1993.

27. Yang, J., and W. Kim, "Analogue to Digital Converter Architecture with a Signal Level Detector," *Electronics Letter*, vol. 30, no. 1, pp.2-3, Seoul, 1994.

28. Hein, S., and A. Zakhor, "Stability and Scaling of Double Loop Sigma-Delta Modulators," *IEEE Proceedings*, pp. 1312-1315, Berkeley, 1992.

29. Tan, N., and S. Eriksson, "Fourth-Order Two-Stage Delta-Sigma Modulator Using Both One Bit and Multi-Bit Quantisers," *Electronics Letters*, vol. 29, no. 11, pp. 937-938, Linkoping, Sweden, 1993.

30. Aziz, P., et al. "Multiband Sigma-Delta Modulation," *Electronics Letters*, vol. 29, no. 9, pp. 760-762, Philadelphia, 1993.

31. Stehwien, W., Radar Systems Engineering, Litton Systems Canada Ltd., (E-mail message), 26 May 1995.

32. Davidson, G. W., et al. "An Approach For Improved Processing in Squint Mode SAR," *International Geoscience and Remote Sensing Symposium Proceedings*, vol. 3, pp. 1173-1175, 1993.

33. Moreira, A., and Y. Huang, "Airborne SAR Processing of Highly Squinted Data Using a Chirp Scaling Approach With Integrated Motion Compensation," *IEEE Transactions on Geoscience and Remote Sensing*, vol. 32, no.5, pp. 1029-1040, 1994.

34. Chen, H.C., and C.D. McGillem, "Target Motion Compensation By Spectrum Shifting in Synthetic Aperture Radar," *IEEE Transactions on Aerospace and Electronic Systems*, vol. 28, no. 3, pp.895-901, 1992.

35. Chuang, W., and T.S. Huang, "Estimating Rotation Speed From Projections in SAR," *IEEE International Conference on Acoustics, Speech and Signal Processing Proceedings*, vol. 3, pp. 21-24, 1992.

36. Jingwen, L., et al. "Imaging of Moving Targets With SAR Based on Space-time Two Dimensional Signal Processing," *IEEE International Radar Conference Proceedings*, p. 396, 1995.

37. Coe, D.J., and R.G. White, "Moving Target Detection in SAR Imagery: Experimental Results," *IEEE International Radar Conference Proceedings*, p. 644, 1995.

38. Robnett, T.J., and B. Charny, "A High-Speed Synthetic Aperture Radar Processor," *IEEE International Conference on Acoustics, Speech and Signal Processing Proceedings*, vol. 4, pp. 357-360, 1992.

39. Voles, R., "Resolving Revolutions: Imaging And Mapping by Modern Radar," *Electronics and Communication Engineering Journal*, vol. 5, no. 1, pp. 3-12, 1993.

40. Premkumar, A., and J. Purviance, "An Architecture For Real Time Processing of SAR Signals," *IEEE International Symposium on Circuits and Systems Proceedings*, vol. 3, pp.1483-1486, 1992.

41. Bierens, L., "Real-time SAR Activities at TNO Physics and Electronics Laboratory," *IEEE International Geoscience and Remote Sensing Symposium Proceedings*, vol. 3, pp.1413-1415, 1993.

42. Dall, J., "A Fast Autofocus Algorithm For Synthetic Aperture Radar Processing," *IEEE International Conference on Acoustics, Speech and Signal Processing Proceedings*, vol. 3, pp. 5-8, 1992.

43. Wahl, D.E., et al. "Phase Gradient Autofocus -- A Robust Tool For High Resolution SAR Phase Correction," *IEEE*

Transactions on Aerospace and Electronic Systems, vol. 30, no. 3, pp. 827-835, 1994.

44. Tunaley, J.K., et al. "Use of The Dempster-Shafer Algorithm in the Detection of Ship Wakes From Synthetic Aperture Radar Images," *IEEE International Conference on Acoustics, Speech and Signal Processing Proceedings*, vol. 4, pp. 2605-2608, 1991.

45. Vachon, P.W., and R.K. Raney, "Ocean Waves And Optimal SAR Processing: Don't Adjust The Focus!" *IEEE Transactions on Geoscience and Remote Sensing*, vol. 30, no.3, pp. 627-630, 1992.

46. Ouchi, K., and D.A. Burridge, "Resolution of a Controversy Surrounding The Focusing Mechanisms of Synthetic Aperture Radar Images of Ocean Waves," *IEEE Transactions on Geoscience and Remote Sensing*, vol. 32, no. 5, pp. 1004-1016, 1994.

47. Baras, J.S., and S.I. Wolk, "Efficient Organization of Large Ship Radar Databases Using Wavelets and Structured Vector Quantization," *Conference Record of The Twenty-seventh Asilomar Conference on Signals, Systems and Computers*, vol. 1, pp. 491-498, 1993.

48. Fechner, T., and R. Tanger, "A Hybrid Neural Network Architecture for Automatic Object Recognition," *Proceedings of the IEEE Workshop on Neural Networks for Signal Processing IV.*, pp. 187-194, 1994.

49. Radiant Outlaw/LADAR presentation slides and data sheets, Autonetics Division of Rockwell Defense Electronics, 1991 & 1995.

50. Dipietro, R.C., "Extended Factored Space-Time Processing for Airborne Radar Systems," *Conference Record of The Twenty-sixth Asilomar Conference on Signals, Systems and Computers*, vol. 1, pp. 425-430, 1992.

51. Barile, E.C., et al. "Some Limitations on the Effectiveness of Airborne Adaptive Radar," *IEEE Transactions on Aerospace and Electronic Systems*, vol. 28, no. 4, pp. 1015-1032, 1992.

52. Fante, R.L., et al. "Clutter Covariance Smoothing by Subaperture Averaging," *IEEE Transactions on Aerospace and Electronic Systems*, vol. 30, no. 3, pp. 941-945, 1994.

53. Richardson, P.E., "Analysis of the Adaptive Space-time Processing Technique For Airborne Radar," *IEE Proceedings - Radar, Sonar and Navigation*, vol. 141, no. 4, pp. 187-195, 1994.

54. Farina, A., and L. Timmoneri, "Space-Time Processing for AEW Radar," *Proceedings of the IEE International Radar Conference*, pp. 312-315, 1992.

55. Wang, H., et al. "Recent Results in Space-Time Processing," *Record of the IEEE National Radar Conference*, pp. 104-109, 1994.

56. Wang, H., and L. Cui, "On Adaptive Spatial-Temporal Processing for Airborne Surveillance Radar Systems," *IEEE Transactions on Aerospace and Electronic Systems*, vol. 30, no. 3, pp. 660-669, 1994.

57. Brennan, L.E., et al. "Comparison of Space-Time Adaptive Processing Approaches Using Experimental Airborne Radar Data," *Record of the IEEE National Radar Conference*, pp. 176-181, 1993.

58. Wicks, M., et al. "Space-Time Adaptive Processing in Modern Electronic Warfare Environments," *Proceedings of the IEEE International Radar Conference*, pp. 609-613, 1995.

59. Caldwell, S.P., et al. "Recent Advances in Exciter and Waveform Generator Technology at Westinghouse," *Record of the IEEE National Radar Conference*, pp. 40-45, 1993.

60. Collier, D.C., "Ferroelectric Phase Shifters for Phased Array Radar Applications," *Proceedings of the Eighth IEEE International Symposium on Applications of Ferroelectrics*, pp. 199-201, 1992.

61. Shnitkin, H., "Joint STARS Phased Array Radar Antenna," *IEEE Aerospace and Electronics Systems Magazine*, vol. 9, no. 10, pp. 34-40, 1994.

62. Tang, C.H., "Effects of Phased Array Structure Deformation and Element Outage," *Digest of IEEE Antennas and Propagation Society International Symposium*, vol. 3, pp. 1608-1611, 1992.

63. Liu, S.C., "A Fault Correction Technique for Phased Array Antennas," *Digest of IEEE Antennas and Propagation Society International Symposium*, vol. 3, pp. 1612-1615, 1992.

64. Babu, B.N.S., and T.P. Guella, "Effects of Antenna Aircraft Interaction on Phased-array Radar Performance," *IEE Proceedings - Radar and Navigation*, vol. 141, no. 5, pp. 279-284, 1994.

65. McIntosh, R.E., et al. "FOPAIR: A Focused Array Imaging Radar for Ocean Remote Sensing," *IEEE Transactions on Geoscience and Remote Sensing*, vol. 33, no. 1, pp. 115-124, 1995.

66. Blake, B., ed., *Jane's Radar and Electronic Warfare Systems*, Jane's Information Group Limited, Surrey, 1995.

67. Blake, B., ed., *Jane's Radar and Electronic Warfare Systems*, Jane's Information Group Limited, Surrey, 1994

68. Tirado, R., and I. Newberg, "Application of Digital Fiber Optics Technology to a Radar Unit-to-unit Cable," *Proceedings of IEEE/AIAA 10th Digital Avionics Systems Conference*, pp. 446-470, 1991.

69. Gowan, J., *Optical Communications Systems*, Prentice/Hall International, p. 18, 1984.

70. Stilwell, D., et al. "Microwave Time Delay Beamforming Using Optics," *Proceedings of the IEEE National Radar Conference*, pp. 50-53, 1991.

71. Lillesand, T.M., and R.W. Kiefer, *Remote Sensing and Image Interpretation, Second Edition*, New York, John Wiley and Sons, 1987.

72. Numnonda, T., and M. Andrews, "High Resolution Image Reconstruction Using Mean Field Annealing," *IEEE Proceedings of the Neural Networks for Signal Processing IV Workshop*, pp. 441-450, 1994.

73. Mukai, Y., and H. Kimura, "The Results of Performance Test of JERS-1 OPS Data," *1993 International Geoscience and Remote Sensing Symposium, Better Understanding of Earth Environment*, pp. 888-890., Vol.2, IEEE, New York, 1993

74. Lecureux, Y., "Optical Sensors and Data Transmission," *IEE Colloquium on 'Earth Resource Sensing and the Data Relay Satellite', Digest No.53*, pp. 3/1-3/15, London, 1990.

75. Levien, F., "Reconnaissance Satellites: Help to Guarantee World Peace," *Professional Careers*, pp. 10-12, January/February, 1989.

76. Crisis Management Satellite, MIT Report No. 3, 1978

77. Witt, M., "Optronics - Scratching the Surface of Possibilities," *Asian Defense Journal*, pp. 65-70, November 1992.

78. Ghosh, S.K., and P.J. Galeski, "Criteria for Selection of Infrared Camera System," *Conference Record of the Industry Applications Conference Twenty-ninth IAS Annual Meeting*, vol. 3, pp. 1893-1897, 1994.

79. Blackman, S.S., et al. "Multiple Hypothesis Track Confirmation for Infrared Surveillance Systems," *IEEE Transactions on Aerospace and Electronic Systems*, vol. 29, no. 3, pp. 810-824, 1993.

80. Peignet, C., et al. "T/R Modules for Phased-Array Antennas," *Proceedings of the IEEE National Radar Conference*, pp.63-66, New York, 1991.

81. Nordwall, B.D., "Millimeter-Wave Radar Tested as Landing Aid," *Aviation Week and Space Technology*, pp. 55-56, May 15, 1995.

82. Gildea, K., "U.S.-NATO Agree to Upgrade AWACS Radar System," *Defense Daily*, p.263, August 23, 1995.

83. (News Breaks), *Aviation Week and Space Technology*, p. 19, June 5, 1995.

84. Oliveri, F., "Air Force Sticks to JSTARS Plan," *Defense Daily*, August 15, 1995.

85. Morrocco, J.D., "Joint-STARS Team Formed For NATO Bid," *Aviation Week and Space Technology*, p. 30, June 19, 1995.

86. (News Breaks), *Aviation Week and Space Technology,* p. 18, May 5, 1995.

87. Nordwall, B.D., "Filter Center," *Aviation Week and Space Technology*, p. 53, March 22, 1993.

114

88. Isnard, J., "Maritime Surveillance -- The French Answer," *Asian Defense Journal*, pp. 63-66, August, 1991.

89. Green, R.O., et al. "On-Orbit Calibration of the Japanese Earth Resources Satellite-1 Optical Sensor Using the Airborne Visible-Infrared Imaging Spectrometer," *International Geoscience and Remote Sensing Symposium Proceedings*, vol. 3, pp. 1312-1314, 1993.

90. Erlich, J., "Merger Creates Research Giant," *Defense News*, p. 11, July 3-9, 1995, Army Times Publishing Company, Springfield, Va.

91. *Defense News*, p. 13, July 10-16, 1995, Army Times Publishing Company, Springfield, Va.

APPENDIX: STATE-OF-THE-ART PERFORMANCE SUMMARY

This table summarizes the performance of the components adressed in the body of the thesis.

Hardware	Performance
T/R modules	single chip: 24.8 mm², 40% PAE, 7 Watts, 200,000 hrs MTBF
Magnetrons	CFA: 10MW peak/100kW avg. @ 1 GHz, 100,000 hrs MTBF ESA noise: 0.7-4 dB @ 0.4-14 GHz
Klystrons	gridded pulse: 6kW avg., 10% BW alloy doped: 95MW peak/3MW avg. @ 1 GHz, 20,000 hrs MTBF
TWTs	700kW @ 1.3 GHz, 4.5MW @ 5.6 GHz
ADCs	optical: 14 bits @ 20 MHz integrated optical: 4 bits @ 1.2 GHz
Exciters	DDS: <-145 dBc/Hz @ 1 kHz additive noise
Antennas	AESAs with up to 2000 T/R modules
Connectors	LiNbO₃ modulator: 3-7 dB insertion noise TTD beamsteering: mrad accuracy
Photo-graphic Cameras	6" resolution @ 248 miles
IR sensors	TE cooling: 50,000 hrs MTBF sensitivity: 0.1°c

118

INITIAL DISTRIBUTION LIST

1. Defense Technical Information Center..................2
    Cameron Station
    Alexandria, Virginia 22304-6145

2. Library, Code 52.....................................2
    Naval Postgraduate School
    Monterey, California 93943-5101

3. The International Radar Directory....................1
    Steven L. Johnston, Editor-in-Chief
    4015 Devon St., S.E.
    Huntsville, Alabama 35802

4. Wolfgang Stehwien, Ph.D., P.Eng.....................1
    Radar Systems Engineering
    Litton Systems Canada Limited
    25 City View Drive, Etobicoke
    Ontario, CANADA M9W 5A7

5. Superintendent......................................7
    Naval Postgraduate School
    Attn. Professor Phillip E. Pace
    Code EC/Pc
    Monterey, California, 93943-5106

6. Superintendent......................................2
    Naval Postgraduate School
    Attn. Professor D. Collins, Chairman
    Code AA/Co
    Attn. Professor O. Biblarz
    Code AA/Bi
    Monterey, California, 93943-5106